NASA Contractor Report 144877

AN INVESTIGATION OF DRAG REDUCTION FOR TRACTOR TRAILER VEHICLES

Vincent U. Muirhead

University of Kansas Center for Research, Incorporated
Lawrence, Kansas

October 1978

NASA Grant NSG-4009

National Aeronautics and
Space Administration

TABLE OF CONTENTS

		Page
TABLE OF CONTENTS		iii
LIST OF SYMBOLS		v
LIST OF FIGURES		vii
LIST OF TABLES		ix
ACKNOWLEDGMENTS		x
SUMMARY		xi
1.	INTRODUCTION	1
2.	APPARATUS AND PROCEDURE	2
	2.1 Models	2
	2.2 Mounting	3
	2.3 Tests	3
3.	RESULTS AND DISCUSSION	4
	3.1 Drag	4
	3.2 Side Force	8
	3.3 Lift	9
	3.4 Pitching Moment	9
	3.5 Rolling Moment	9
	3.6 Yawing Moment	10
4.	CONCLUSIONS AND RECOMMENDATIONS	10
5.	REFERENCES	12
6.	FIGURES AND TABLES	13
7.	APPENDIX	50

LIST OF SYMBOLS

A	Projected frontal area on a plane perpendicular to the centerline of the truck, scaled from A value from reference 7
C_D	Coefficient of drag, D/qA
C_L	Coefficient of lift, L/qA
C_M	Coefficient of pitching moment, PM/qAc
C_Y	Coefficient of side force, SF/qA
C_ℓ	Coefficient of rolling moment, RM/qAc
C_N	Coefficient of yawing moment, YM/qAc
C_{D_X}	Coefficient of drag, configuration X
C_{P_b}	Coefficient of base pressure, $(P_b - P_A)/q$
c	Reference length (vehicle length for C_M) (vehicle width for C_ℓ, C_Y)
D	Drag (truck axis)
D_e	Equivalent diameter, $\sqrt{4A/\pi}$
L	Lift (truck axis)
P	Power
P_A	Atmospheric pressure
P_b	Base pressure
PM	Pitching moment (truck axis)
q	True dynamic pressure in wind tunnel test section, $1/2\ \rho V^2$
RM	Rolling moment (truck axis)
R_N	Reynolds number (based on equivalent diameter), $\rho V D_e/\mu$
SF	Side force (truck axis)
V	Relative wind speed = Wind tunnel airspeed

V_1	Vehicle speed
V_2	Side wind component
W	True wind speed
YM	Yawing moment (truck axis)
β	Wind angle relative to vehicle path
ρ	Air density
μ	Air viscosity
ψ	Yaw angle = Relative wind angle

LIST OF FIGURES

Figure		Page
2.1.1	Full-scale basic vehicle	13
2.1.2	Full-scale vehicle with and without forward streamlining	14
2.1.3	Forward streamlining - full-scale	15
2.1.4	Model configuration chart	16
2.1.5	Photographs of wind tunnel model configurations. . .	17
2.2.1	Wind tunnel mount.	21
3.1.1	Reynolds number effect on drag coefficient, C_{D_1} . . .	22
3.1.2	Effect of wind angle on drag coefficient, C_{D_1}. . . .	23
3.1.3	Comparison of drag coefficients, configuration 1, 2, 3, 4, 5, 6, 7	24
3.1.4	Flow over rounded front - 0° yaw	25
3.1.5	Flow over streamlined rear - 0° yaw	26
3.1.6	Flow at 30° yaw - vortex forming	27
3.1.7	Reynolds number effect on base pressure coefficient, $C_{P_{b_1}}$	28
3.1.8	Effect of wind angle on base pressure coefficient, $C_{P_{b_1}}$	29
3.1.9	Comparison of base pressure coefficients, configuration 1, 2, 3, 4, 5, 6, 7	30
3.1.10	Power required to overcome aerodynamic drag, configuration 1.	31
3.1.11	Power required to overcome aerodynamic drag, configuration 7	32
3.2.1	Reynolds number effect on side force coefficient C_{Y_1}	33
3.2.2	Effect of wind angle on side force coefficient, C_{Y_1}	34

3.2.3 Comparison of side force coefficients, configuration 1, 2, 3, 4, 5, 6, 7. 35

3.3.1 Reynolds number effect on lift coefficient, C_{L_1}. . . 36

3.3.2 Effect of wind angle on lift coefficient, C_{L_1}. . . . 37

3.4.1 Reynolds number effect on pitching moment coefficient C_{M_1}. 38

3.4.2 Effect of wind angle on pitching moment coefficient, C_{M_1} 39

3.5.1 Reynolds number effect on rolling moment coefficient, $C_{\ell 1}$ 40

3.5.2 Effect of wind angle on rolling moment coefficient, C_{ℓ_1} 41

3.6.1 Reynolds number effect on yawing moment coefficient, C_{N_1} 42

3.6.2 Effect of wind angle on yawing moment coefficient, C_{N_1} 43

LIST OF TABLES

Table		Page
I	Full-scale basic vehicle characteristics	44
II	Drag coefficients, $R_N = 6 \times 10^5$.	44
III	Influence on the drag coefficient by configuration changes	45
IV	Comparison of tests run at Dryden Flight Research Center and the University of Kansas.	45
V	Pressure coefficients, $R_N = 6 \times 10^5$	46
VI	Side force coefficients, $R_N = 6 \times 10^5$.	46
VII	Influence on the side force coefficient by configuration changes.	47
VIII	Lift coefficients, $R_N = 6 \times 10^5$.	47
IX	Pitching moment coefficients, $R_N = 6 \times 10^5$	48
X	Rolling moment coefficients, $R_N = 6 \times 10^5$.	48
XI	Yawing moment coefficients, $R_N = 6 \times 10^5$	49

ACKNOWLEDGMENTS

The advice and comments of Mr. Edwin Saltzman, Dryden Flight Research Center, are gratefully acknowledged. The wind tunnel testing and data reduction were conducted by the following students in the Department of Aerospace Engineering, University of Kansas:

Charles A. Hughes, M.S. candidate

Carl Kulp, M.S. candidate

Steven Ericson, Undergraduate student

Michael R. Griswold, Undergraduate student

Don Markow, Undergraduate student

Charles Vaughan, Undergraduate student

SUMMARY

A wind tunnel investigation was conducted to determine the reduction in drag which could be obtained by using certain forward, underbody and rear streamlining on tractor-trailer vehicles. Tests were conducted at yaw angles (relative wind) of 0, 5, 10, 20, and 30 degrees and Reynolds numbers of 3.58×10^5 to 6.12×10^5 based upon the equivalent diameter of the vehicles.

The significant results were:

1. The forward streamlining of the tractor and the enclosing of the gap between the tractor and trailer decreased the drag 40.2% of configuration 1 for zero wind. With side winds the average decrease was 33%.

2. The lower panels reduced the drag 8.7% of configuration 1 for zero wind. With side winds the average decrease was 19%.

3. The rear streamlining reduced the drag 4.8% of the configuration 1 for zero wind. With side winds the average decrease was 10%.

4. The aerodynamic drag of the final configuration was 40.4% of the baseline vehicle drag for zero wind. With side winds the average drag was 33% of the baseline vehicle drag.

1. INTRODUCTION

A number of wind tunnel tests have been made on tractor-trailer vehicles with various add-on devices to reduce aerodynamic drag. Sherwood[1] tested a large number of devices. Some of these produced very favorable results. Potter[2] in 1956 patented an "Inflatable Streamlining Apparatus for Vehicle Bodies". Unfortunately, the trucking industry did "not believe that the devices suggested were practical for use". The current fuel oil and energy outlook should make the aerodynamic drag of practical concern. Montoya and Steers[3] conducted full-scale tests in 1974 of a number of add-on devices around the tractor cab area. The maximum drag reduction was approximately 24%. Some devices provided only minor changes. These data were all for zero wind conditions. Also, during 1974 the drag of several box-shaped vehicle configurations was determined by Saltzman, Meyer and Lux[4] by a coast down method. Wind tunnel tests were conducted during 1975 and 1976 on one-tenth scale models of the Saltzman, Meyer and Lux configurations[5] and additional configurations at various wind angles. The significant results of these tests indicated that:

1. Rounding the front corners 19.9% of the effective diameter of the frontal area reduced the drag approximately 58%.
2. A boat tail with a radius equal to the equivalent diameter of the frontal area reduced the drag about 20%.
3. A smooth bottom decreased the drag about 10%.

Subsequently, wind tunnel tests have been conducted at the University of Kansas upon a one-twenty-fifth scale model of the basic tractor trailer vehicle used by Montoya and Steers[3]. Then, a series of modifications were made to the baseline model to improve the air flow over the front, the rear and the underbody of the vehicle. These modifications include and extend those of reference 7. Tests were made at five different wind angles.

2. APPARATUS AND PROCEDURE

2.1 Models

The full-scale vehicle is shown in Figure 2.1.1, and its characteristics are contained in Table 1. Figure 2.1.2 shows the baseline full-scale tractor trailer vehicle together with a vehicle with forward streamlining. Forward streamlining details are shown in Figure 2.1.3.

The baseline wind tunnel model, configuration 1, was constructed from a commercially available one-twenty-fifth scale plastic model kit. This kit closely simulated the important geometric features of the tractor though the trailer had to be lengthened somewhat with balsa-wood to conform to the scaled dimensions of the full-scale trailer. For subsequent configurations, balsa streamlining was added to the baseline model in three steps as indicated in Figure 2.1.4 to form configurations 2, 3 and 4. Configuration 5 was constructed by adding balsa lower side panels which extended below the tractor and trailer of the model to within 1.6 cm. (.63") of the ground. Configuration 6 was made by adding a boat tail, to the model, Figure 2.1.4, which had a radius of 13.7 cm.

(5.39"). A smooth balsa bottom was added to configuration 6 to form configuration 7.

Configurations were assembled according to Figure 2.1.4. Photographs of the models are shown in Figure 2.1.5.

2.2 Mounting

The wind tunnel mounting system for the models, Figure 2.2.1, was the same system that had been used on the previous tests of the box-shaped vehicles[5]. The ground board enclosed the balance mounting strut and mounting plate. The model was held to the mounting plate by six adjustable rods attached to the tractor and trailer frames and running through the wheels. The model was adjusted vertically on the rods to position the model to the correct height above the ground board. The bottom of the wheels were sanded off so that they did not touch the ground board during the tests. The ground board contained three circular slots to allow the model to be rotated thirty degrees in each direction. During the tests the slots were covered except for a small clearance around each mounting rod.

The horizontal pressure gradient on the ground board was zero. The board was tufted to check for flow separation. The front of the ground board was rounded slightly to eliminate a small flow separation at the leading edge.

2.3 Tests

The tests were conducted in the University of Kansas, .91 by 1.29 meter wind tunnel at Reynolds numbers of 3.58×10^5 to 6.12×10^5 based upon the equivalent diameter of the vehicles or 18.64×10^5 to 32.00×10^5 based upon the length of the basic test model, configuration 1. The Reynolds number was controlled

by adjusting the wind tunnel airspeed from 164.2 to 289.8 kilometers per hour (102.0 to 180.1 mph). Tests were made at yaw (relative wind) angles of 0°, 5°, 10°, 20°, and 30° on all configurations at four different Reynolds numbers. Force and moment data were obtained from a six component strain-gaged balance. Base pressures were measured by an alcohol manometer. For configurations 6 and 7 the base pressure orifice was located at the boattail apex.

3. RESULTS AND DISCUSSION

3.1 Drag

Drag coefficients were computed from the force acting on the wind tunnel model along the model axis. These coefficients were plotted as a function of Reynolds number at each yaw angle. Figure 3.1.1 shows the values for configuration 1 which has been used as the baseline configuration. A Reynolds number of 6×10^5 (based upon equivalent diameter) was selected to compare the drag data of the various configurations, Table II. Figure 3.1.2 shows the variation of the drag coefficient with yaw (relative wind) angle at this Reynolds number. Figure 3.1.3 compares the drag coefficients of the seven configurations tested at the various yaw angles for a Reynolds number of 6×10^5. These drag coefficients were normalized by dividing each drag coefficient by the baseline coefficient at each yaw angle.

The drag data included herein and observations made during the tests indicated the following:

1. The effect of Reynolds number on drag was small.

2. Rounding the cab nose, configuration 2, produced a moderate decrease of approximately 4.8% in drag at zero wind relative to configuration 1. With side winds the average decrease was 7%.

3. Adding the cab top, configuration 3, provided an additional decrease of 15.7% in drag at zero wind relative to configuration 2. With side winds the average decrease was only 9%.

4. Adding the gap enclosure, configuration 4, decreased the drag an additional 19.7% relative to configuration 3 at zero wind. Thus, the complete front modification produced a total decrease of 40.2% for zero wind. With side winds the average decrease for the gap enclosure was 17% for an accumulative total of 33%.

5. The lower side panels added to reduce the gap between the underbody and the ground reduced the drag by 8.7% relative to configuration 4 with zero wind. With side winds the average decrease was 19%.

6. The rear boat-tail streamlining reduced the drag by 4.8% relative to configuration 5, for zero wind. With side winds the average decrease was 10%.

7. The smooth bottom, configuration 7, provided a 5.9% decrease in drag relative to configuration 6 at zero wind. With side winds the average decrease was 5%.

8. The total accumulative decrease in drag of configuration 7 was 59.6% at zero wind, and with side winds the average decrease was 67% relative to configuration 1.

All incremental and accumulative drag coefficient decreases are expressed as a percentage of the baseline drag coefficient at the respective relative wind (yaw) angle. A summary of the incremental and the accumulative drag changes as the individual changes were made to the model is contained in Table III. The incremental and the accumulative changes are shown both for the zero wind conditions and, where labeled as average, the average of values representing side winds providing yaw angles from 0 degrees to 20 degrees.

Table IV presents a comparison between the comparable data points obtained at the NASA Dryden Flight Research Center on the full-scale vehicle and the University of Kansas on the wind tunnel

model. It cannot be determined to what extent Reynolds number is a factor in the difference between full scale and model results; small geometric differences in the models tested may also be a factor. It will be noted that the percentage decrease in drag of model configuration 4 over the baseline model (40.2%) is nearly the same as the decrease in the full-scale front enclosure vehicle over the full-scale baseline (36.7%). The ΔC_D decreases are respectively .398 and .43.

Figure 3.1.4 shows the flow over the rounded front of the vehicle at zero yaw angle. The streamlines are traced by neutrally bouyant helium bubbles. Flow over the rear boat-tail streamliner is shown in Figure 3.1.5. Figure 3.1.6 illustrates the large vortex created at a yaw angle (relative wind) of 30°.

The variation of the base pressure coefficients with Reynolds number for configuration 1 is shown in Figure 3.1.7. The variation with yaw angle for a Reynolds number of 6×10^5 is shown in Figure 3.1.8. Table V contains the base pressure coefficients for all configurations at a Reynolds number of 6×10^5. A comparison of the normalized base pressure coefficients for the seven configurations is contained in Figure 3.1.9. The base pressure coefficients of the baseline model at each yaw angle were used as normalizing factors. The base pressure coefficients follow the same general comparison pattern as did the drag coefficients.

The power required to overcome t e aerodynamic drag for a full-scale vehicle, configuration 1, at 88.5 kilometers per hour (55 mph) ground speed was calculated using wind speeds of 0, 18, and 36 kilometers per hour (0, 11.2 and 22.4 mph). Wind angles

of 0° through 180° relative to the vehicle path were used, Figure 3.1.10. The corresponding values for configuration 7 are given in Figure 3.1.11. The power required for aerodynamic drag at 88.5 kilometers per hour (55 mph) ground speed and no wind was reduced from 78.6 kw (105.4 hp) for configuration 1 to 31.8 kw (42.6 hp) for configuration 7. At a wind speed of 18 kilometers per hour (11.2 mph) and β=45° the power required was 127.0 kw (170.3 hp) for configuration 1 and 43.3 kw (58.1 hp) for configuration 7. For a wind speed of 36 kilometers per hour (22.4 mph) and β=45° the values were 204.0 kw (273.6 hp) and 58.5 kw (78.4 hp) respectively.

The power required for the other configurations, exclusive of mechanical losses, may be found from the comparison graph, Figure 3.1.3 and Figure 3.1.10 as illustrated in the appendix.

The approximate fuel and cost savings provided by the decrease in aerodynamic drag of configurations 4 and 7 over configuration 1 are illustrated for two conditions. A normal brake specific fuel consumption of 2.129×10^{-4} kg of fuel per watt hour[6] (.35 pounds of fuel per horsepower hour) has been used. The savings are as follows for a ground speed of 88.5 kilometers per hour (55 mph) and assumed cost for fuel of 13.2 cents per liter (50 cents per gallon):

Wind, β=45° km/hr. (mph)	Config.	Fuel		Cost	Savings
		liters/hr.	gal./hr.	$/hr.	$/hr.
no wind	1	19.7	5.20	2.60	---
	4	11.8	3.11	1.55	1.05
	7	8.0	2.10	1.05	1.55
18 (11.2)	1	31.8	8.40	4.20	---
	4	22.0	5.82	2.91	1.29
	7	10.8	2.86	1.43	2.77

	Config.	---	$/hr.
Assumed average, day-to-day, savings,	4	---	1.10
	7	---	2.00

For 160,900 km. (100,000 mi.) of highway driving per year, the assummed average annual savings project to about $2,000 per year and $3,600 per year for configurations 4 and 7 respectively.

3.2 Side Force

The side force coefficients were computed from the forces acting on the wind tunnel model perpendicular to the model axis. These coefficients were plotted as a function of Reynolds number as illustrated in Figure 3.2.1 for configuration 1. Figure 3.2.2 shows the variation of side force coefficient for configuration 1 with yaw angle at a Reynolds number of 6×10^5. The side force coefficients for a Reynolds number of 6×10^5 corrected for wind tunnel flow angularity error are contained in Table VI for all configurations. A comparison of all configurations is given in Figure 3.2.3.

The data indicated the following:

1. The effect of Reynolds number on side force was small.

2. Rounding the cab nose increased the side force approximately 1% relative to configuration 1. Adding streamlining to the top of the cab increased the side force about 3% relative to configuration 2.

3. The average increase in side force by enclosing the gap between the tractor and trailer was 13%. The total front modification produced a total average increase of 17% in side force relative to configuration 1.

4. The lower side panels increased the side force an average of 32% relative to configuration 4.

5. The rear boat-tail streamlining decreased the side force approximately 1% from configuration 5.

6. The smooth bottom caused negligible change in side force relative to configuration 6. The accumulative average increase in side force of configuration 7 over configuration 1 was 48%.

A summary of the incremental side force changes as individual changes were made to the model is contained in Table VII. The power required to overcome the side force induced tire-frictional drag effects are negligble (reference 5).

3.3 Lift

The variation of the lift coefficient with Reynolds number is shown in Figure 3.3.1 for model configuration 1. The effect of yaw angle is given in Figure 3.3.2. The lift coefficients of all of the configurations (R_N= 6 x 10^5) are given in Table VIII.

The lift force contributes to the vehicle rolling frictional drag through either increasing or decreasing the weight on the tires. This effect is negligible on the power required.[5]

3.4 Pitching Moment

The pitching moment coefficients of model configuration 1 about a lateral axis 27.9 cm (11.0") from the front of the vehicle and 5.7 cm (2.25") above the ground plane are shown in Figure 3.4.1. The reference area used was the projected frontal area A; the reference length c was the vehicle length. The variation of pitching moment coefficient with yaw angle for configuration 1 is shown in Figure 3.4.2. The pitching moment coefficients of all of the configurations are given in Table IX (R_N= 6 x 10^5).

3.5 Rolling Moment

The rolling moment coefficients of model configuration 1 about a central longitudinal axis 5.7 cm (2.23") above the ground plane are shown in Figure 3.5.1. The reference area was the

projected area A; the reference length c was the vehicle width. The variation of rolling moment coefficient with yaw angle for configuration 1 is shown in Figure 3.5.2. The rolling moment coefficients for all configurations corrected for flow angularity error (see Figures 3.5.1 and 3.5.2) are given in Table X ($R_N = 6 \times 10^5$).

3.6 Yawing Moment

The yawing moment coefficients for the model of configuration 1 about a central vertical axis 27.9 cm (11.0") from the front of the vehicle are shown in Figure 3.6.1. The reference area used was the projected frontal area A; the reference length c was the vehicle width. The variation of the yawing moment with yaw angle for configuration 1 is shown in Figure 3.6.2. The yawing moment coefficients for all of the configurations corrected for flow angularity error (see Figures 3.6.1 and 3.6.2) are given in Table XI ($R_N = 6 \times 10^5$).

4. CONCLUSIONS AND RECOMMENDATIONS

The significant conclusions were:

1. The streamlining of the front of the vehicle and the enclosing of the gap between the tractor and the trailer (configuration 4) decreased the drag 40.2% of configuration 1 for zero wind. With side winds the average decrease was 33%.

2. The lower side panels decreased the drag 8.7% of configuration 1 for zero wind. With side winds the average decrease was 19%.

3. The rear streamlining decreased the drag 4.8% of configuration 1 for zero wind. With side winds the average decrease was 10%.

4. The smooth bottom decreased the drag 5.9% for zero wind. With side winds the average decrease was 5%.

5. The aerodynamic drag of configuration 7 was 40.4% of that of configuration 1 for zero wind. With side winds the average value of drag for configuration 7 was 33% of the drag for configuration 1.

It is recommended that:

1. A program be initiated to road test in an operational fleet configurations 1 and 7 under as nearly identical conditions as possible to evaluate actual savings that would occur in normal usage of a vehicle.

2. State laws be revised to permit the added length at the rear of the vehicle needed for streamlining the rear. This additional length would be for the installation of an inflatable or removable device such as patented by Potter[2]. This would permit the savings on highway operation and the shorter normal length in city areas in which the added length is undesirable.

5. REFERENCES

1. Sherwood, Wiley A., "Wind Resistance" University of Maryland, 1957.
2. Potter, R.D., "Inflatable Streamlining Apparatus for Vehicle Bodies," U.S. Patent No. 2, 737, 411, March 6, 1956.
3. Montoya, Lawrence C. and Steers, Louis L., "Aerodynamic Drag Reduction Tests on a Full-Scale Tractor-Trailer Combination with Several Add-on-Devices," NASA TM X-56028, December 1974.
4. Saltzman, Edwin J., Meyer, Robert R., Jr., and Lux, David P., "Drag Reductions Obtained by Modifying a Box-Shaped Ground Vehicle," NASA TM X-56027, October, 1974.
5. Muirhead, Vincent U., "An Investigation of Drag Reduction on Box-Shaped Ground Vehicles," KU-FRL 180, July, 1976.
6. Diesel & Gas Turbine Worldwide Catalog, 1976 edition, Volume #1, Publication and Circulation Headquarters, P.O. Box 138, 105 Washington Avenue, Oshkosh, Wis. 54901.
7. Steers, Louis L. and Saltzman, Edwin J., "Reduced Truck Fuel Consumption through Aerodynamic Design," Journal of Energy, Vol. 1 No. 5, Sept. - Oct. 1977.

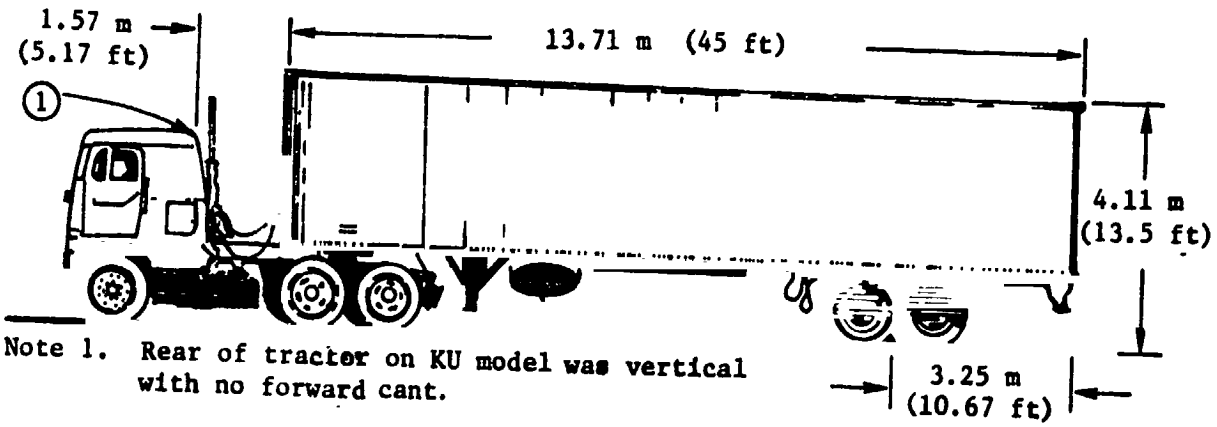

Note 1. Rear of tractor on KU model was vertical with no forward cant.

(a) Side view.

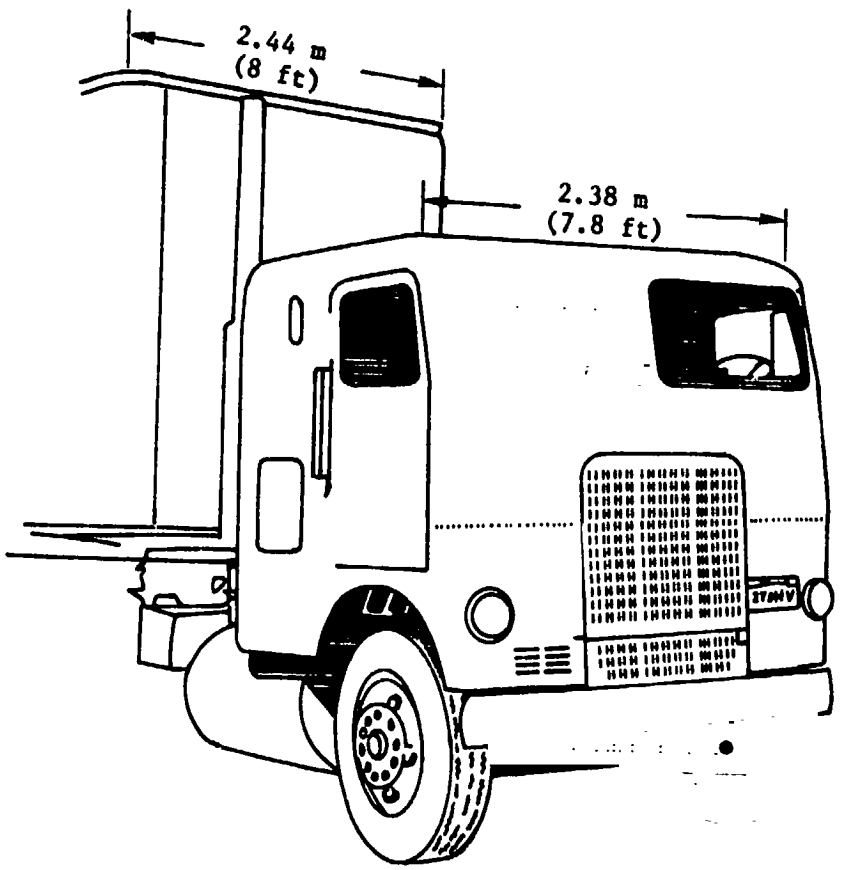

(b) Three-quarter front view.

Figure 2.1.1 Full-scale Basic Vehicle of references 3 and 7.

Figure 2.1.2 Full-scale Vehicle With and Without Forward Streamlining, reference 7.

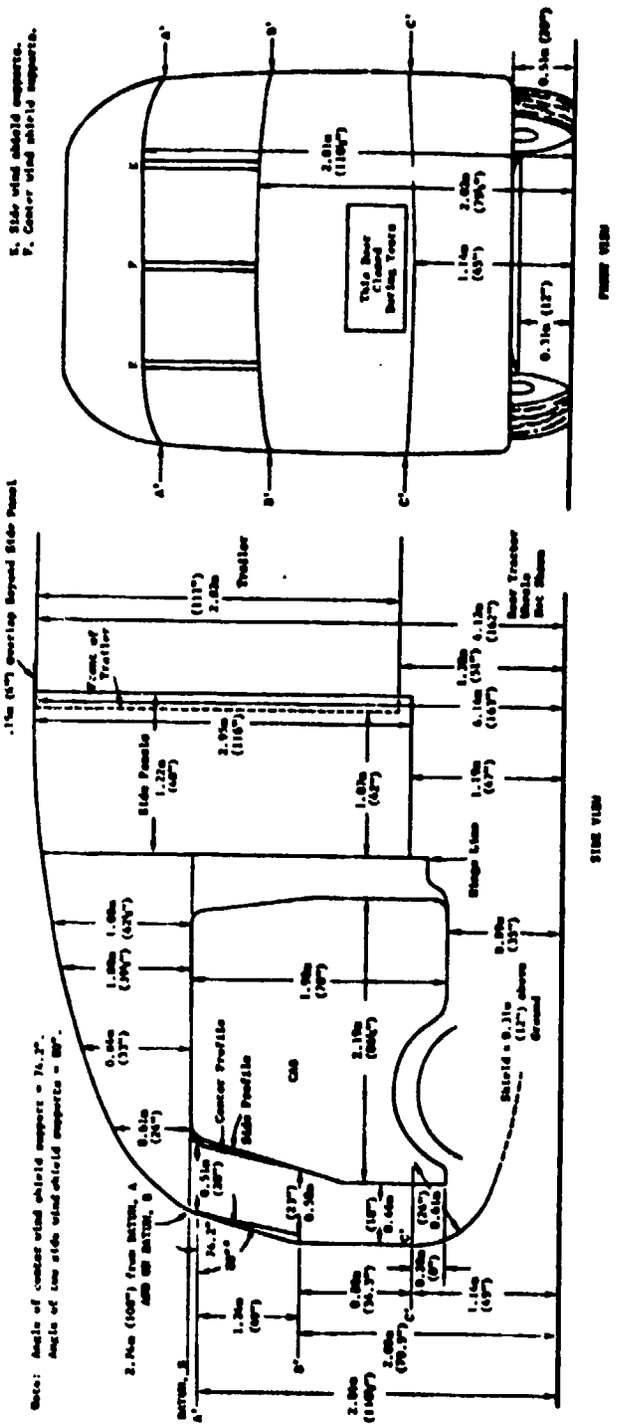

Figure 2.1.3. Forward Streamlining - Full-scale, as in reference 7.

CONFIGURATIONS

No.	Cab	Trailer	Cab nose	Cab top	Gap enclosure (top and sides)	Lower side panels	Rear	Bottom (cab and trailer)
1	Baseline	Baseline	□	□	None	None	□	Rough
2	Modified	Baseline	◖	□	None	None	□	Rough
3	Modified	Baseline	◖	◿	None	None	□	Rough
4	Modified	Baseline	◖	◿	Yes	None	□	Rough
5	Modified	Modified	◖	◿	Yes	Yes	□	Rough
6	Modified	Modified	◖	◿	Yes	Yes	◗	Rough
7	Modified	Modified	◖	◿	Yes	Yes	◗	Smooth

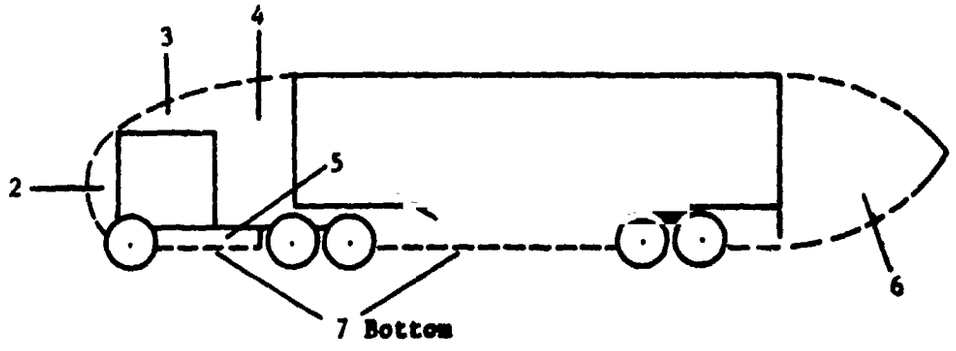

Figure 2.1.4 Model Configuration Chart

(a) Configuration 1

Figure 2.1.5 Photographs of Wind Tunnel Model Configurations

(b) Configuration 2

Figure 2.1.5 Photographs of Wind Tunnel Model Configurations (continued)

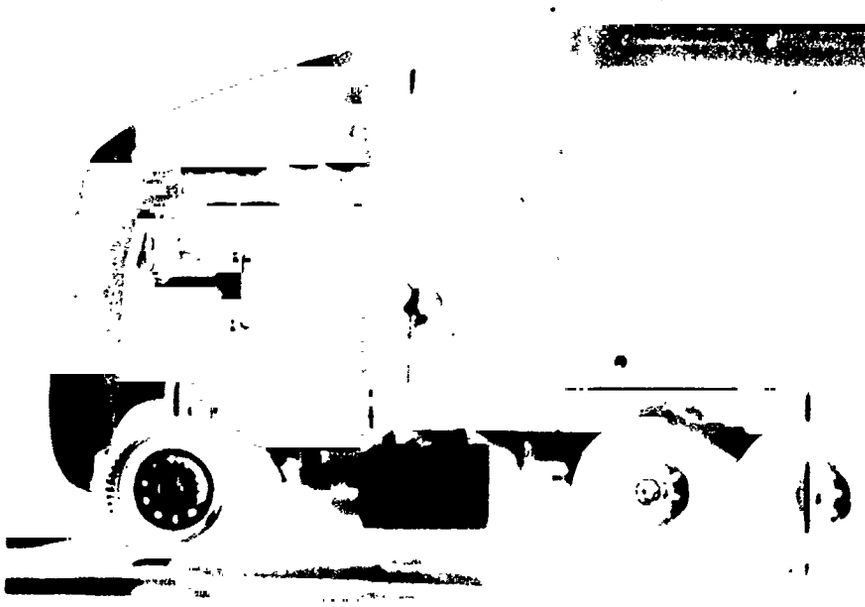

(c) Configuration 3

Figure 2.1.5 Photographs of Wind Tunnel Model Configurations (continued)

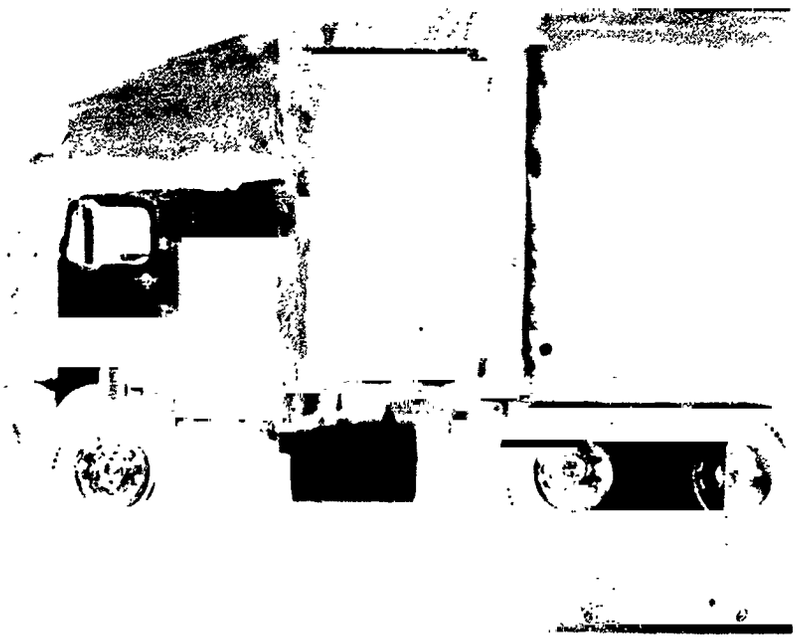

(d) Configuration 4

Figure 2.1.5 Photographs of Wind Tunnel Model Configurations (continued)

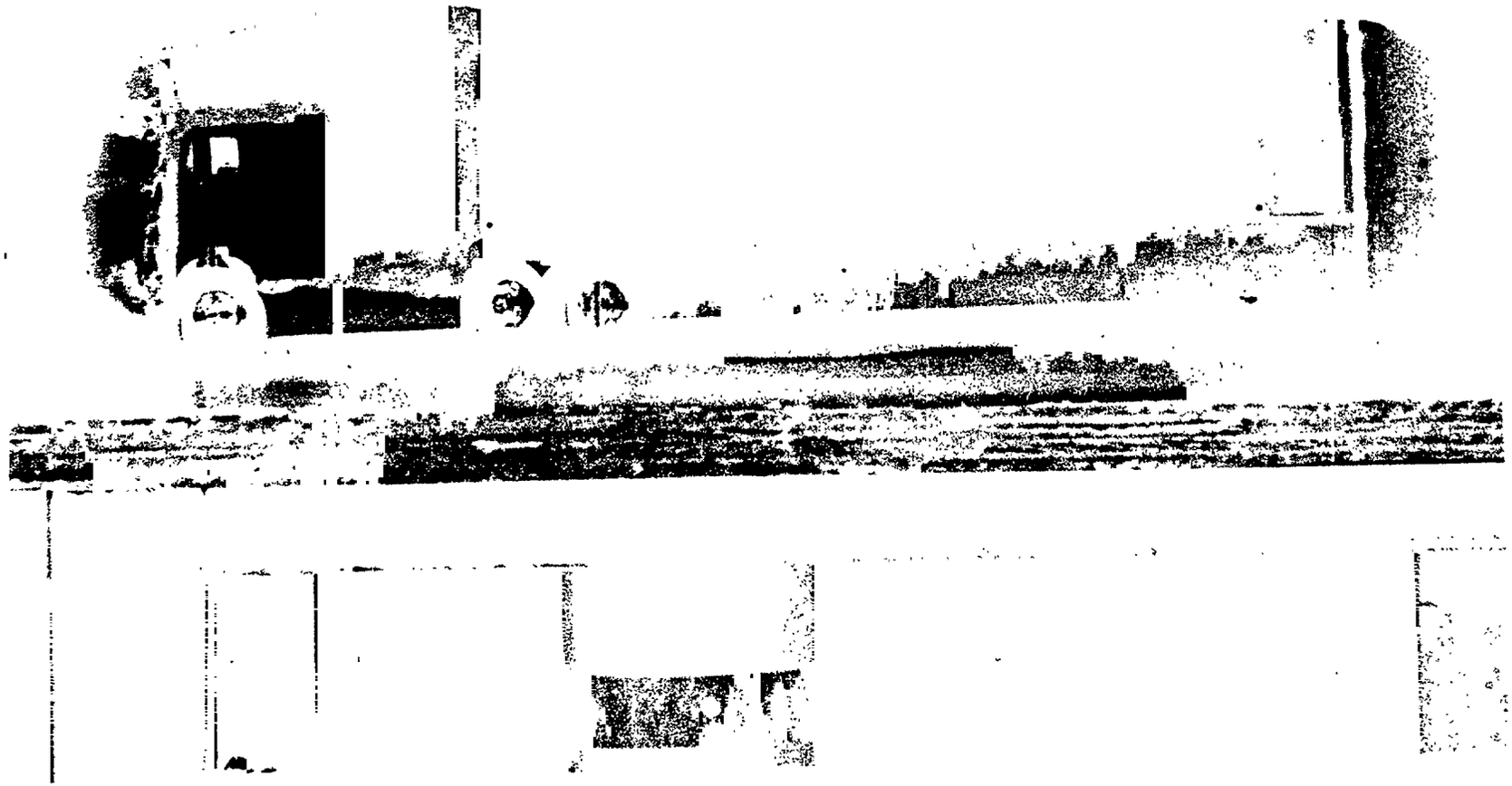

(e) Configuration 7

Figure 2.1.5 Photographs of Wind Tunnel Model Configurations (continued)

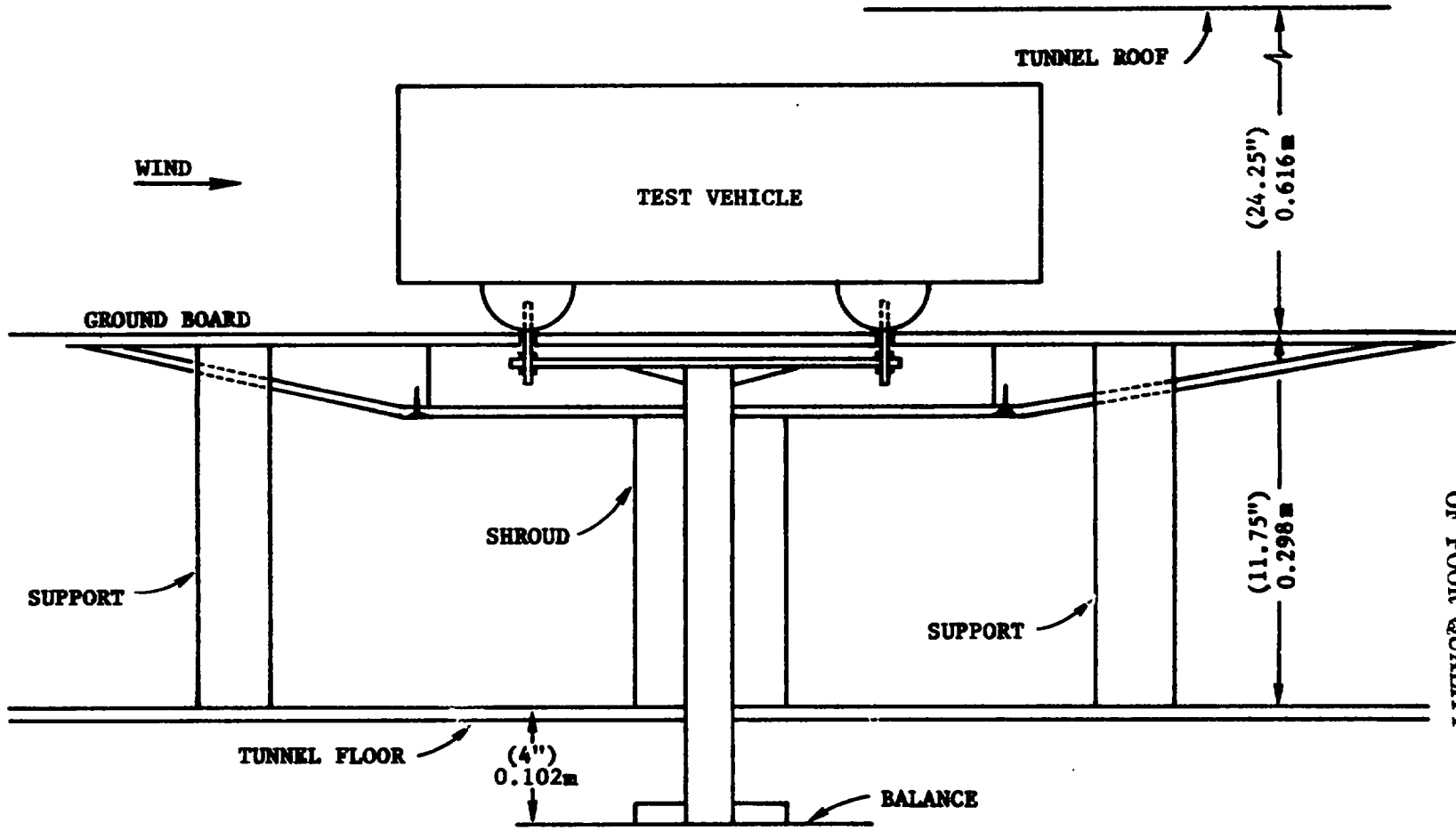

Figure 2.2.1 Wind Tunnel Mount

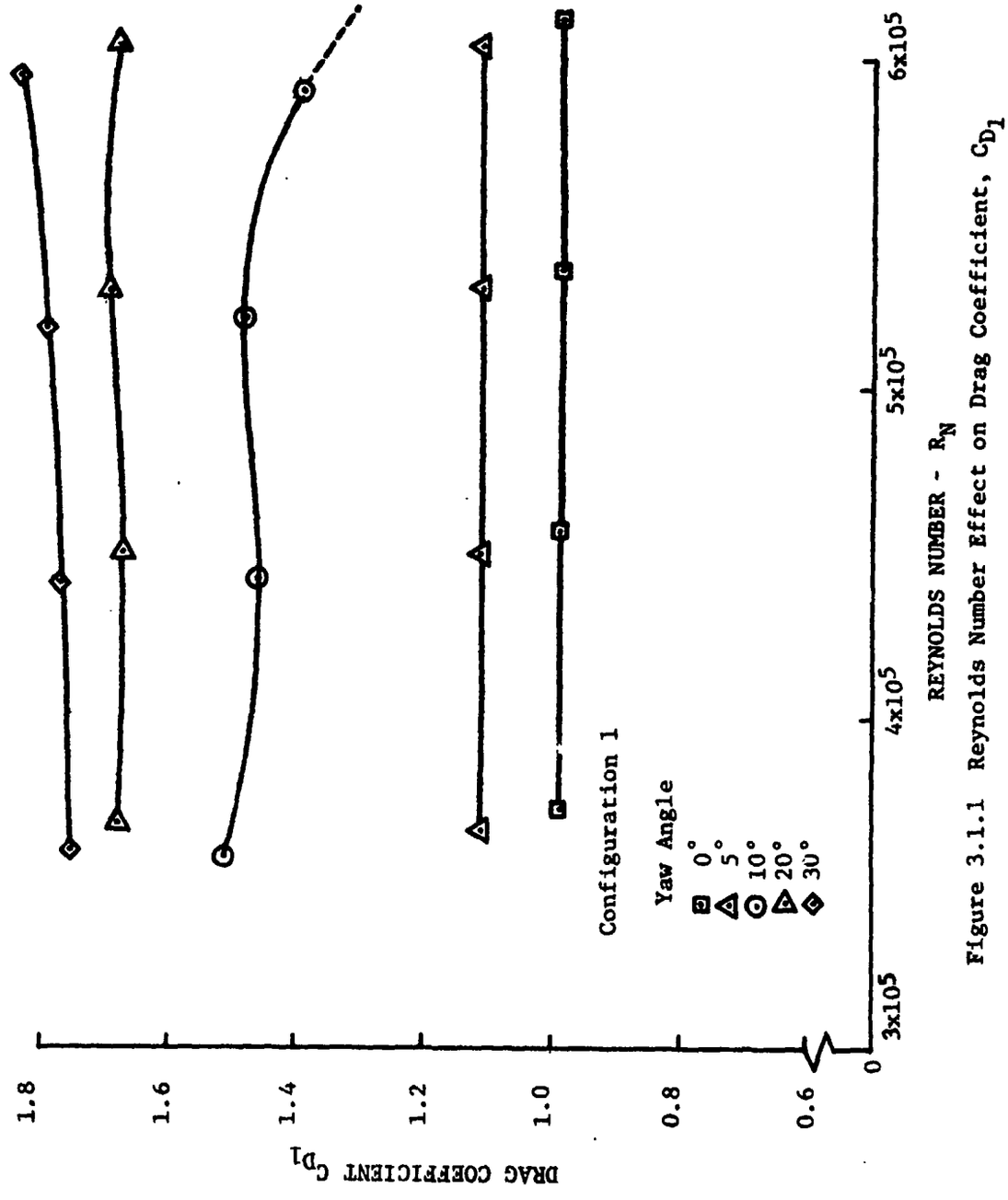

Figure 3.1.1 Reynolds Number Effect on Drag Coefficient, C_{D_1}

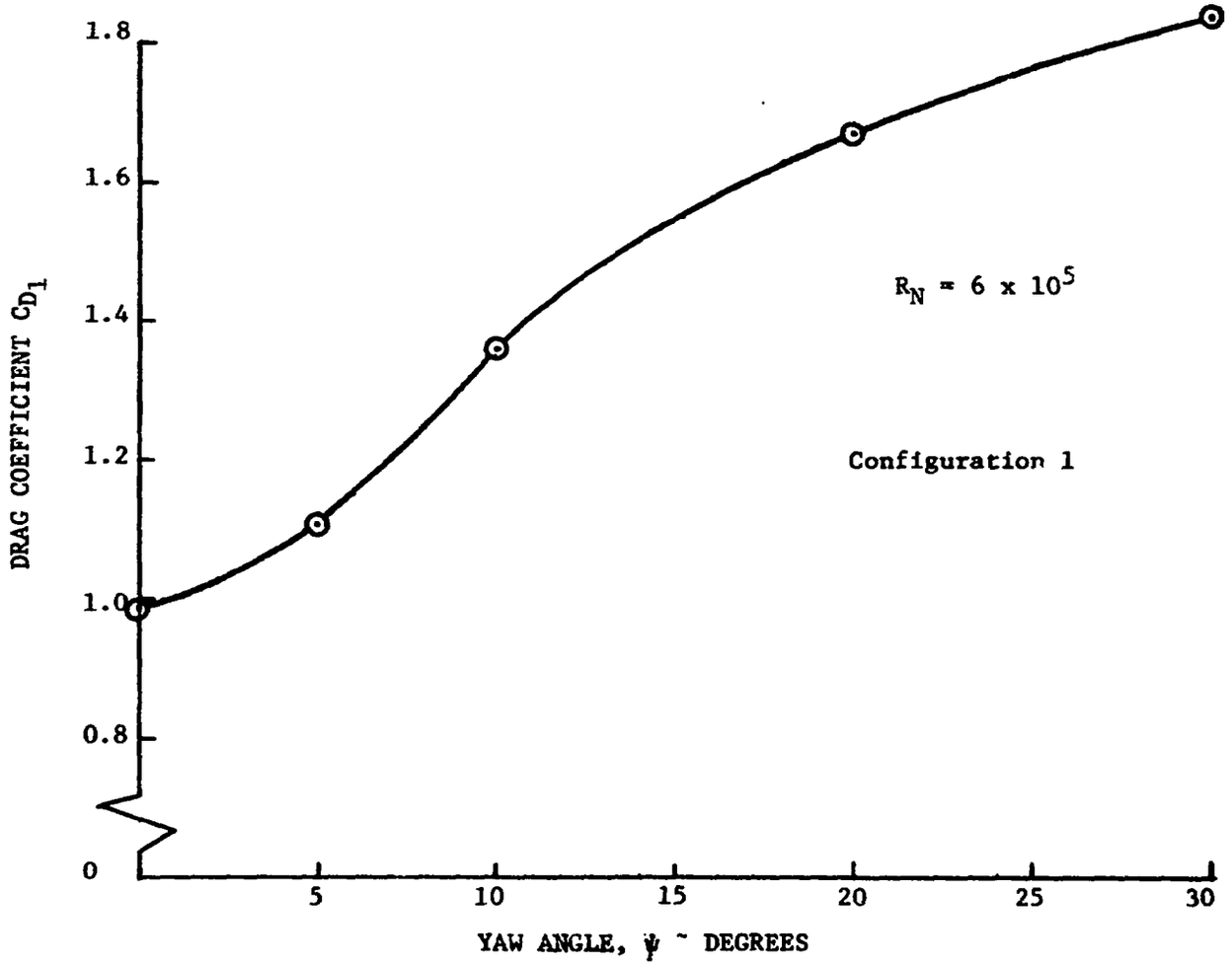

Figure 3.1.2 Effect of Wind Angle on Drag Coefficient, C_{D_1}

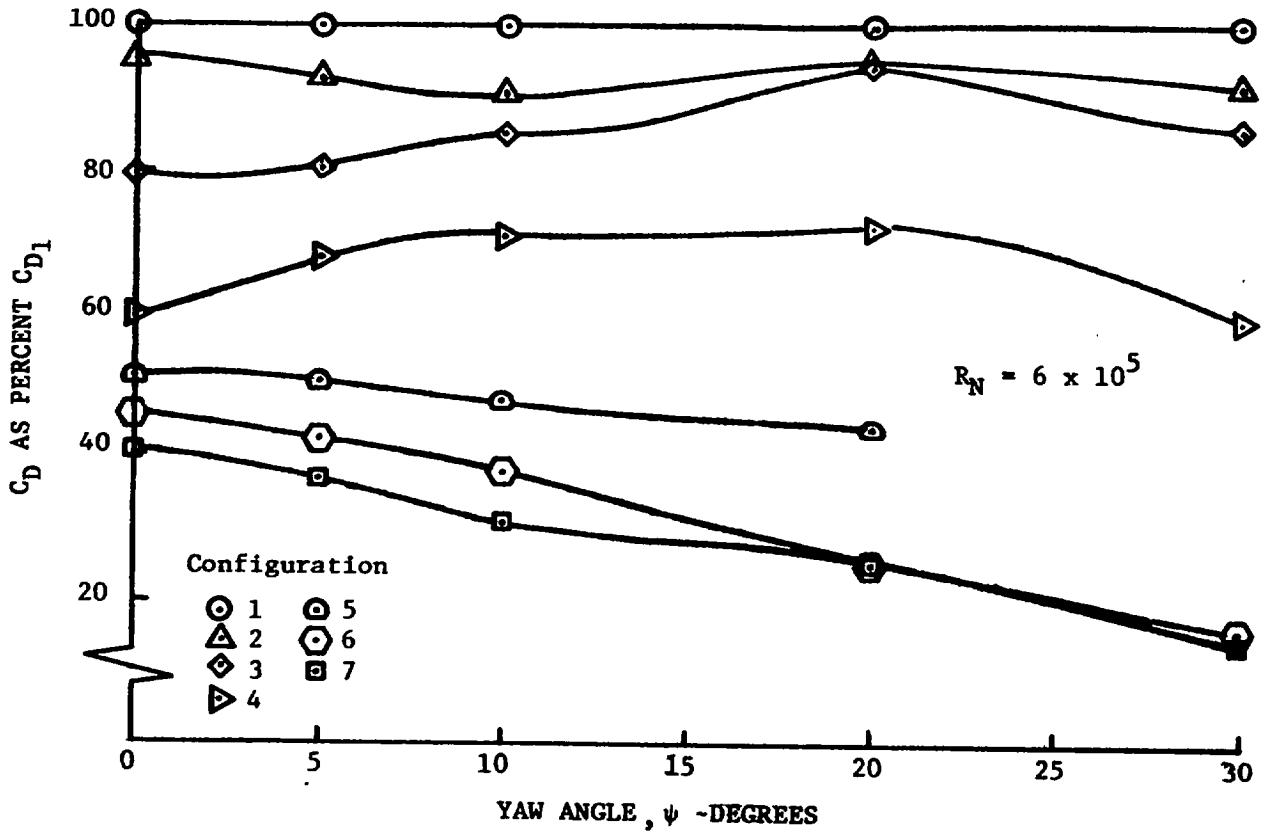

Figure 3.1.3 Comparison of Drag Coefficients, Configuration 1, 2, 3, 4, 5, 6, 7

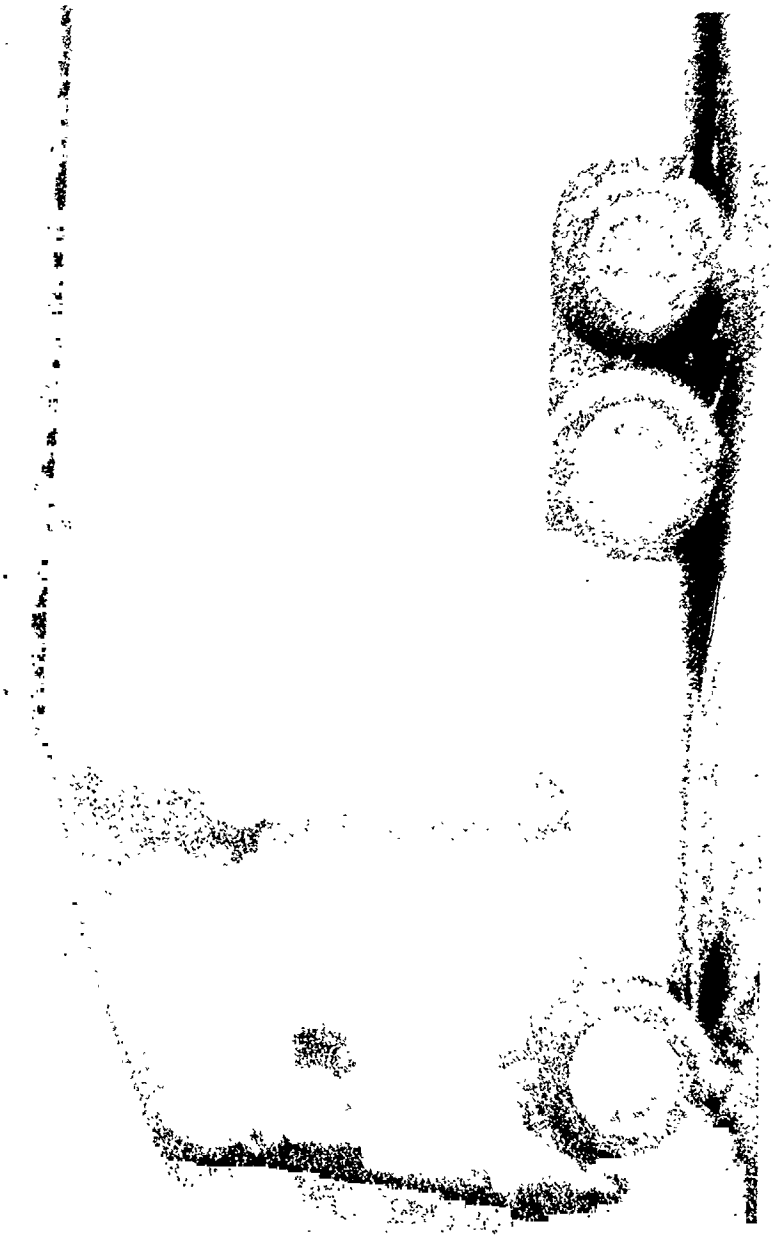

Figure 3.1.4 Flow Over Rounded Front - 0° Yaw

Figure 3.1.5 Flow Over Streamlined Rear - 0° Yaw

Figure 3.1.6 Flow at 30° Yaw - Vortex Forming

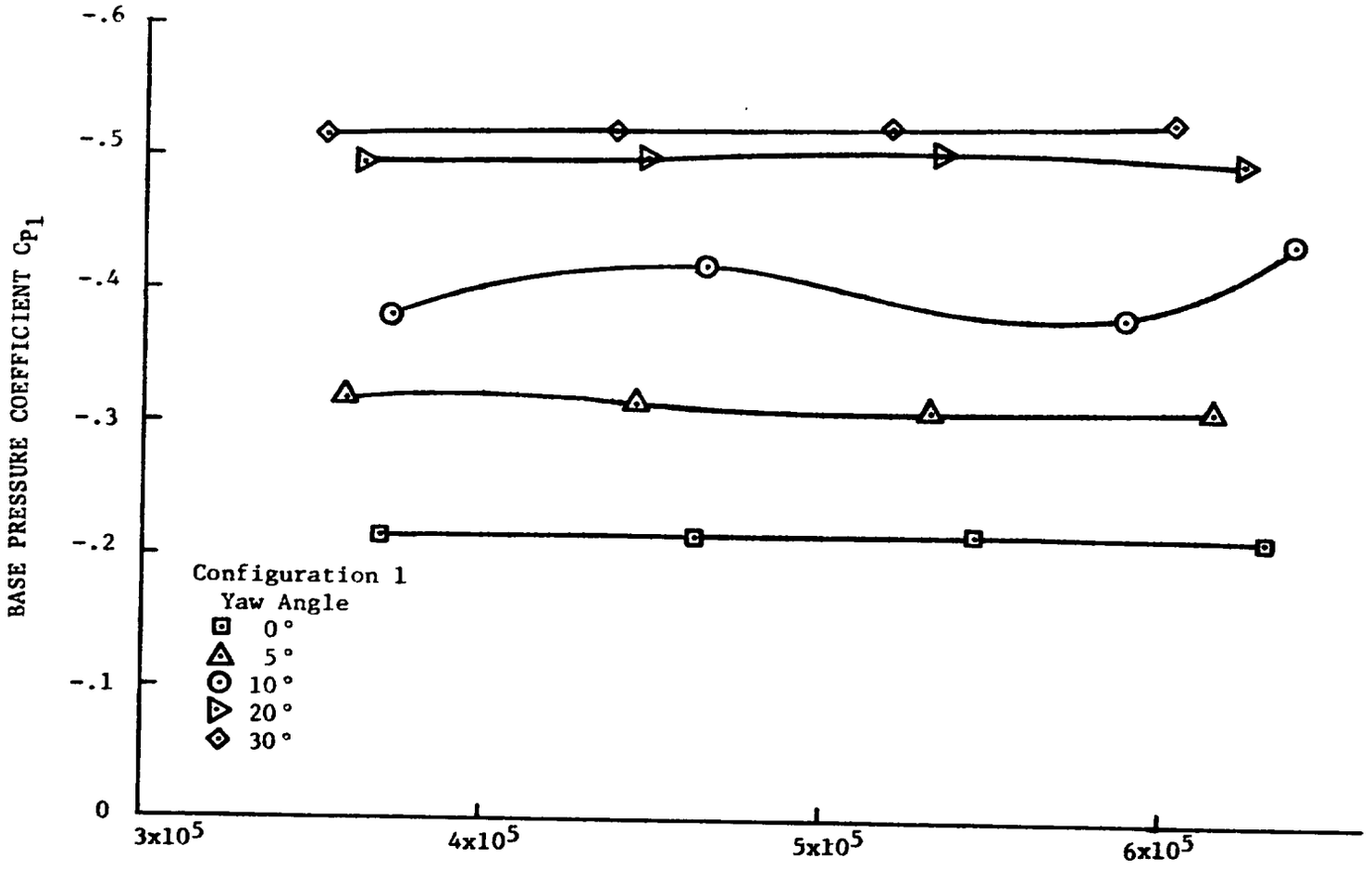

Figure 3.1.7 Reynolds Number Effect on Base Pressure Coefficient C_{P_1}

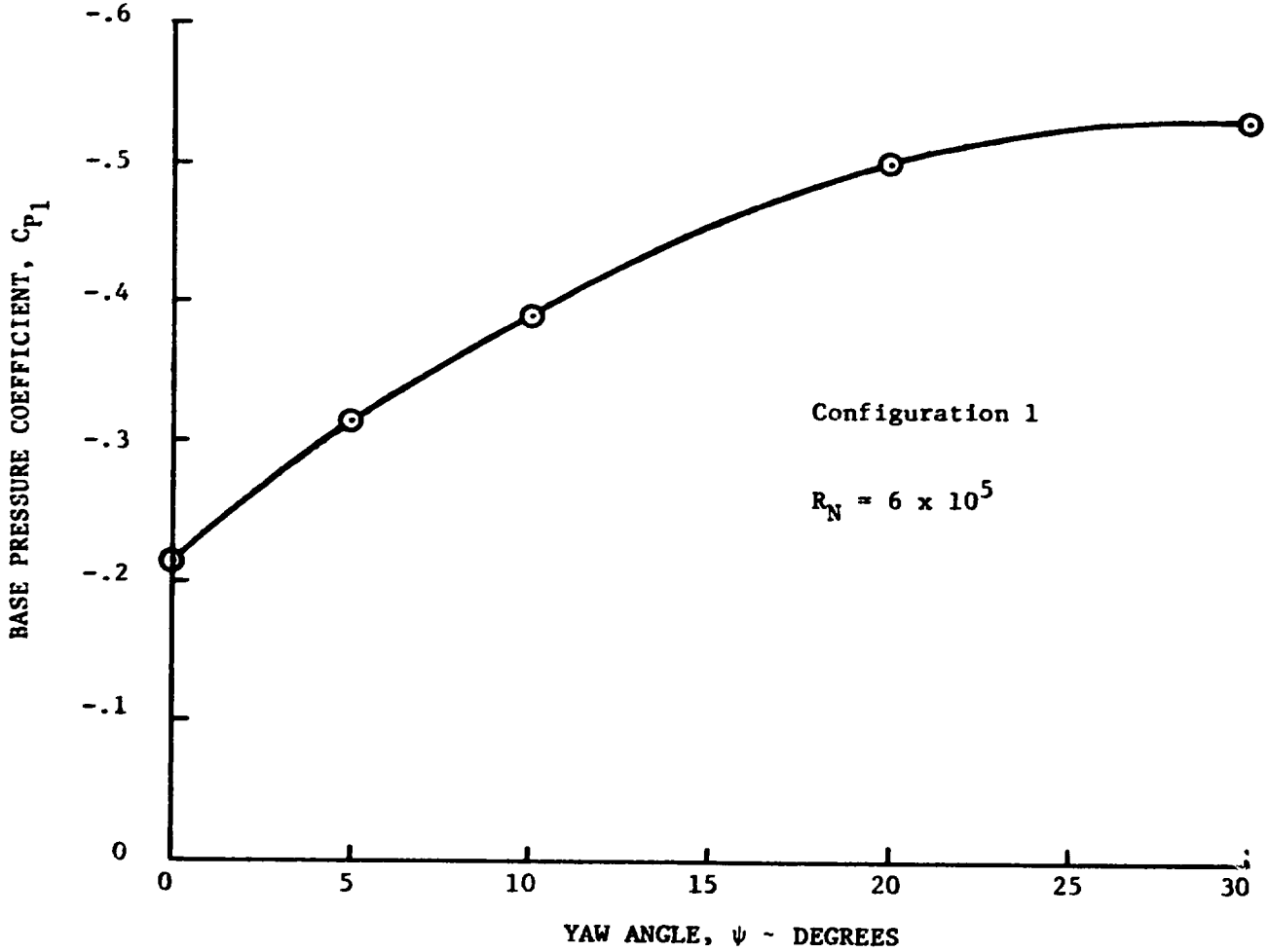

Figure 3.1.8 Effect of Wind Angle on Base Pressure Coefficient, C_{P_1}

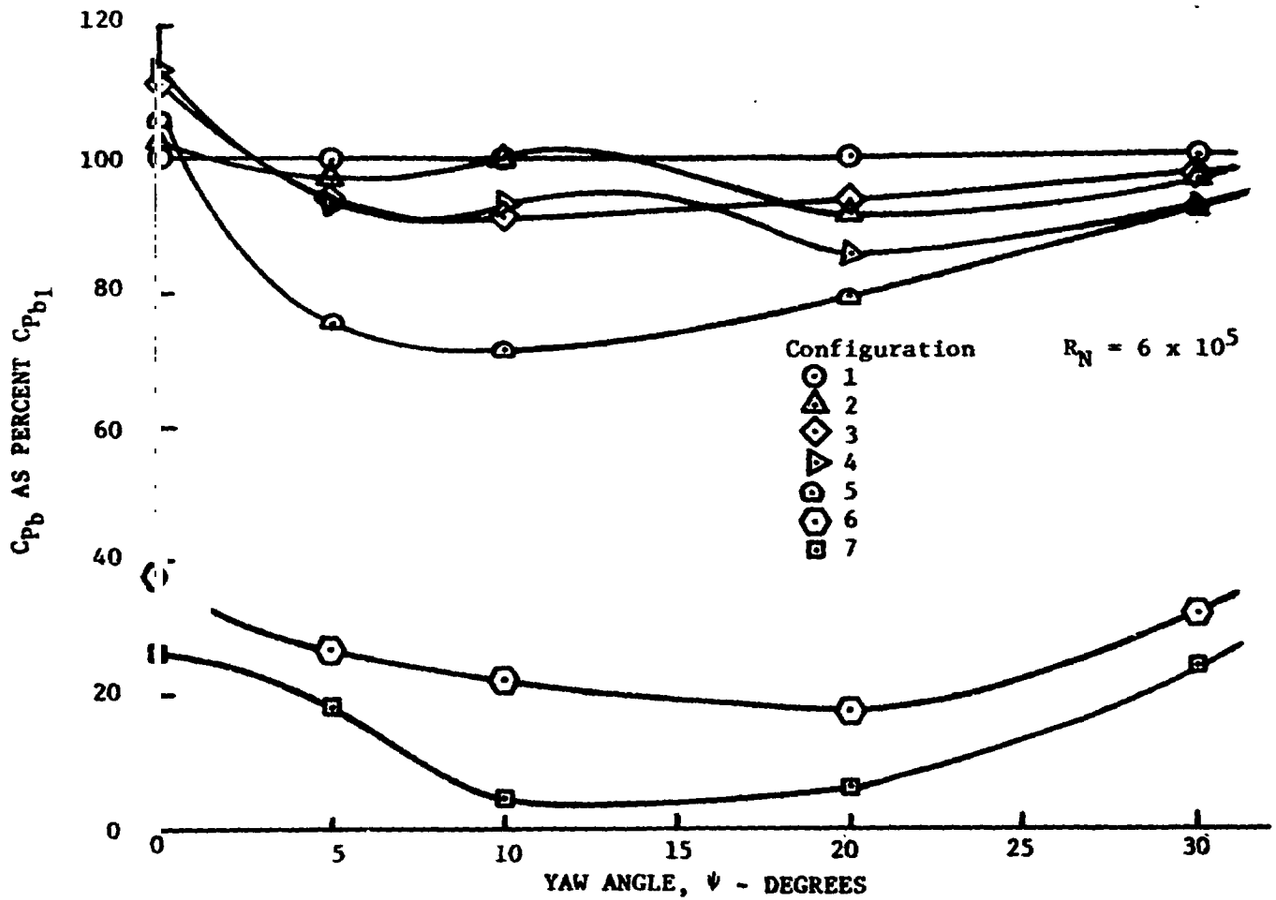

Figure 3.1.9 Comparison of Base Pressure Coefficients, Configuration 1, 2, 3, 4, 5, 6, 7

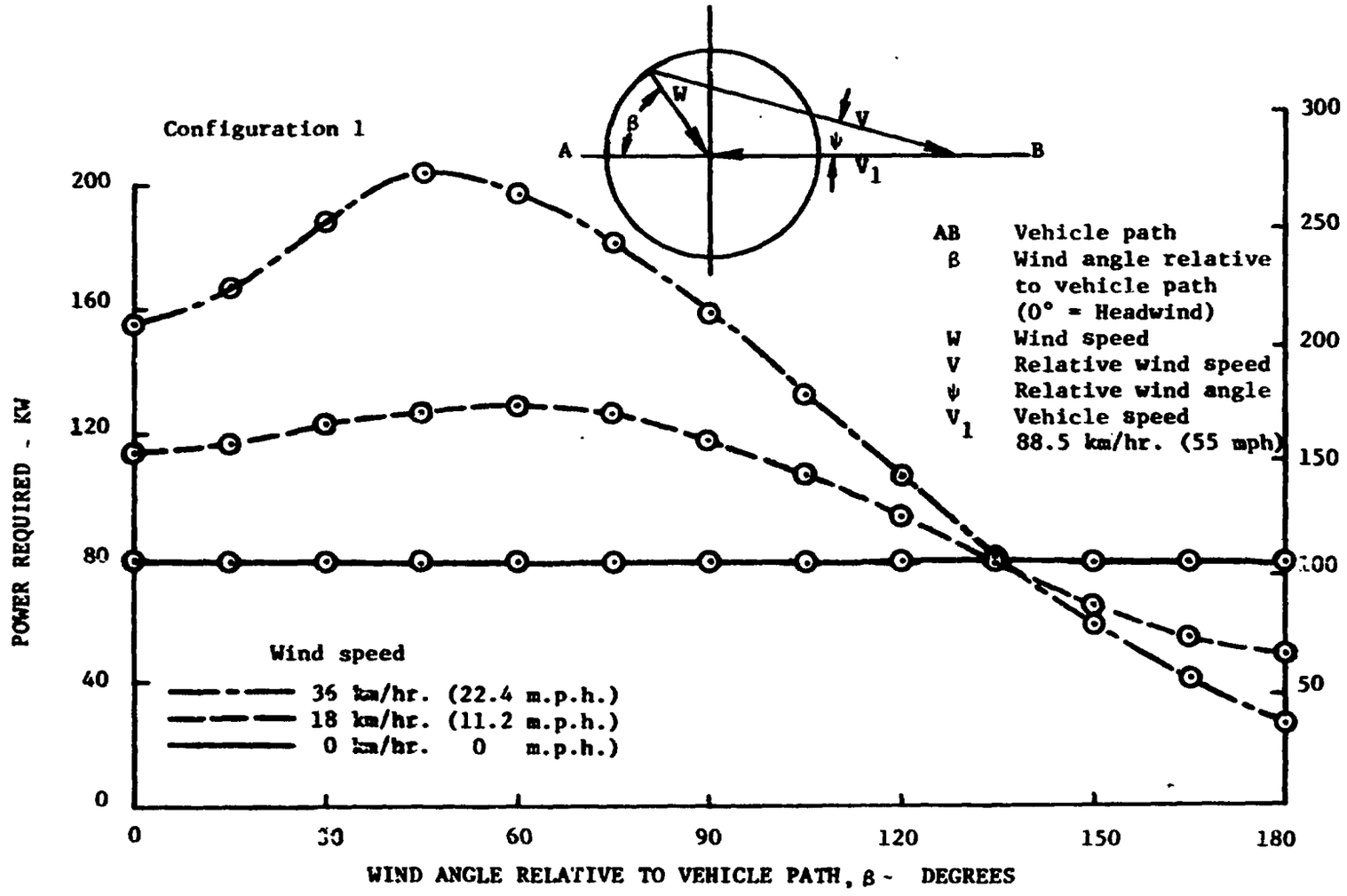

Figure 3.1.10 Power Required to Overcome Aerodynamic Drag, Configuration 1

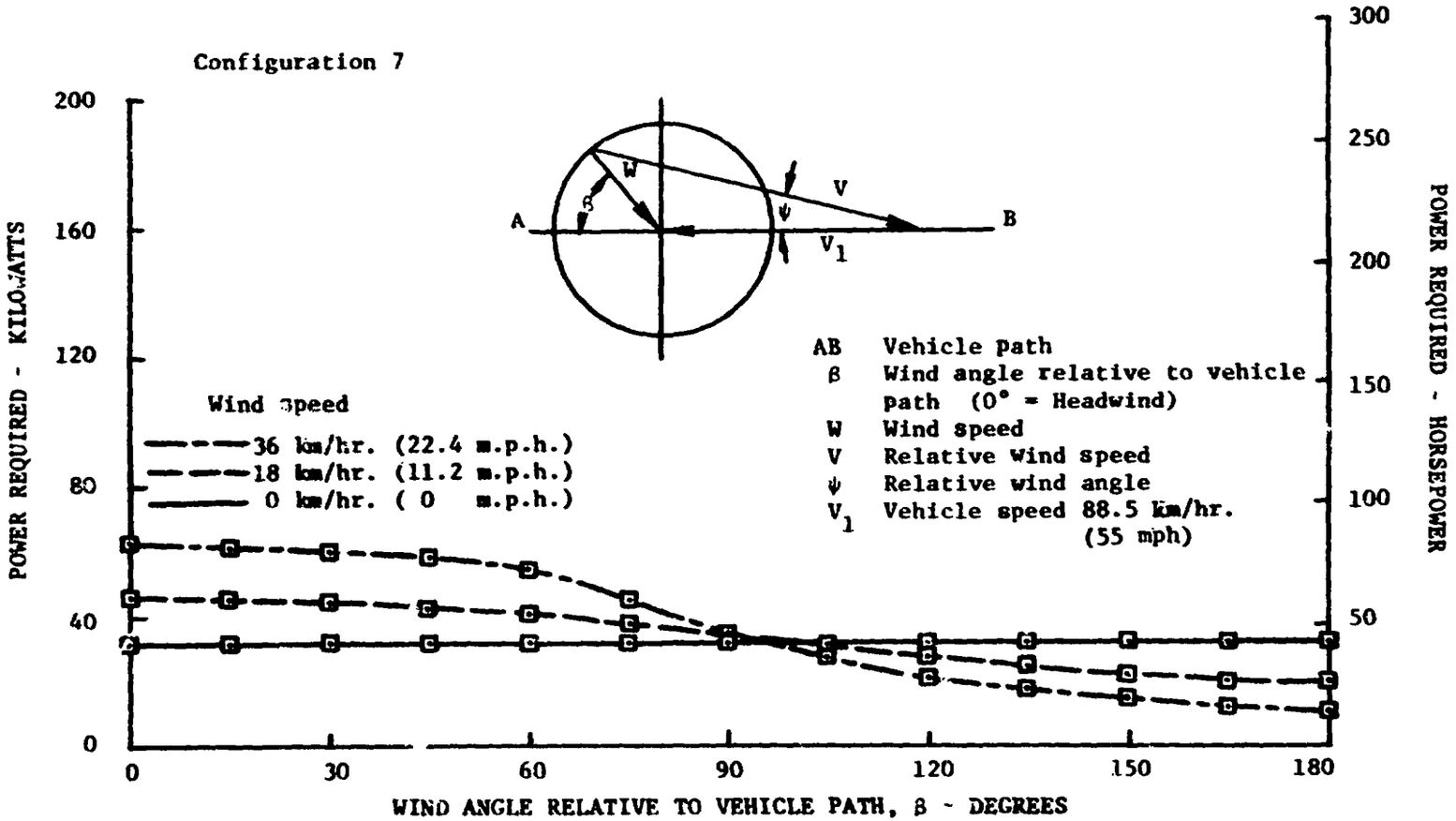

Figure 3.1.11 Power Required to Overcome Aerodynamic Drag, Configuration 7

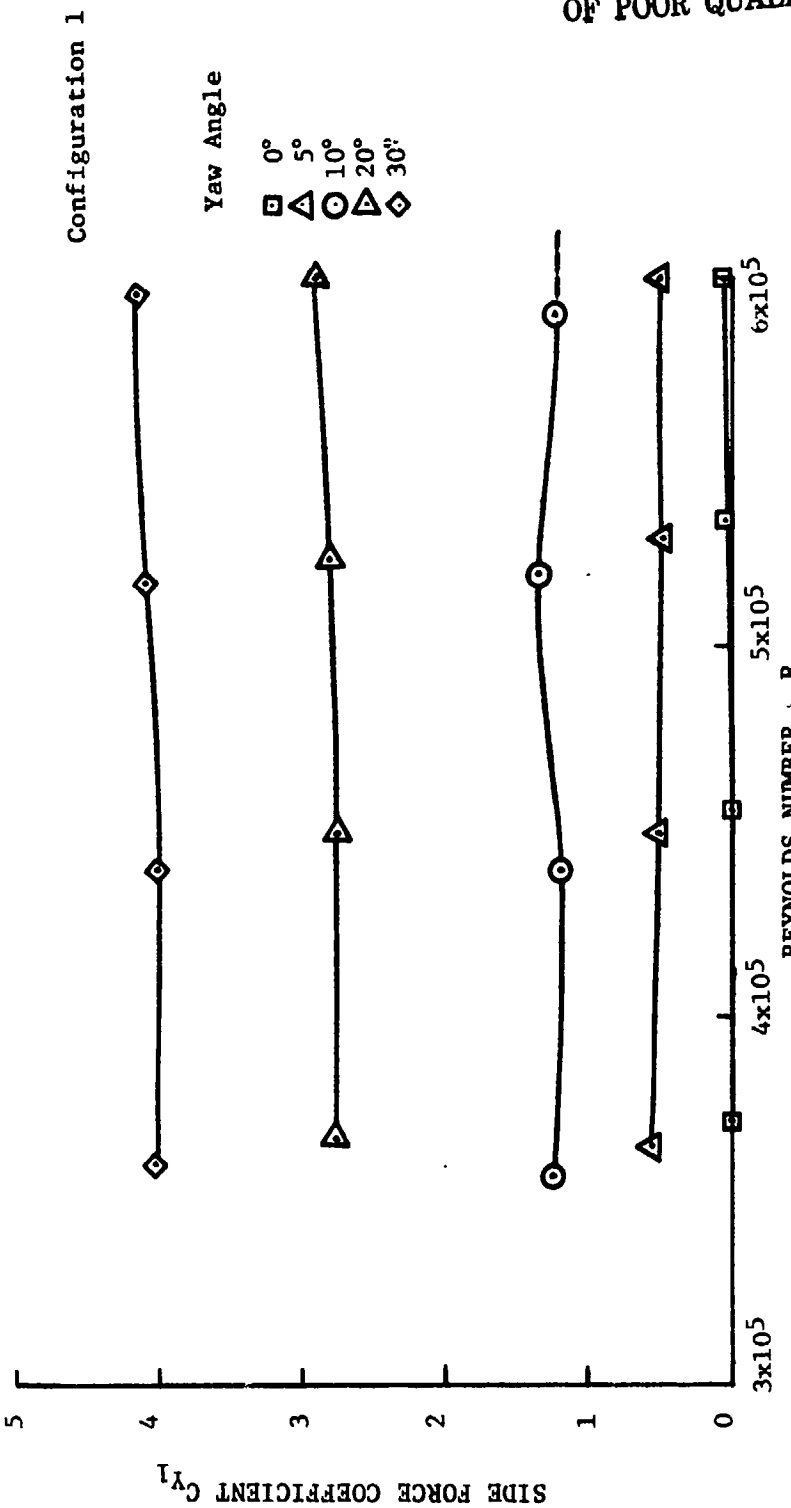

Figure 3.2.1 Reynolds Number Effect on Side Force Coefficient, C_{Y_1}

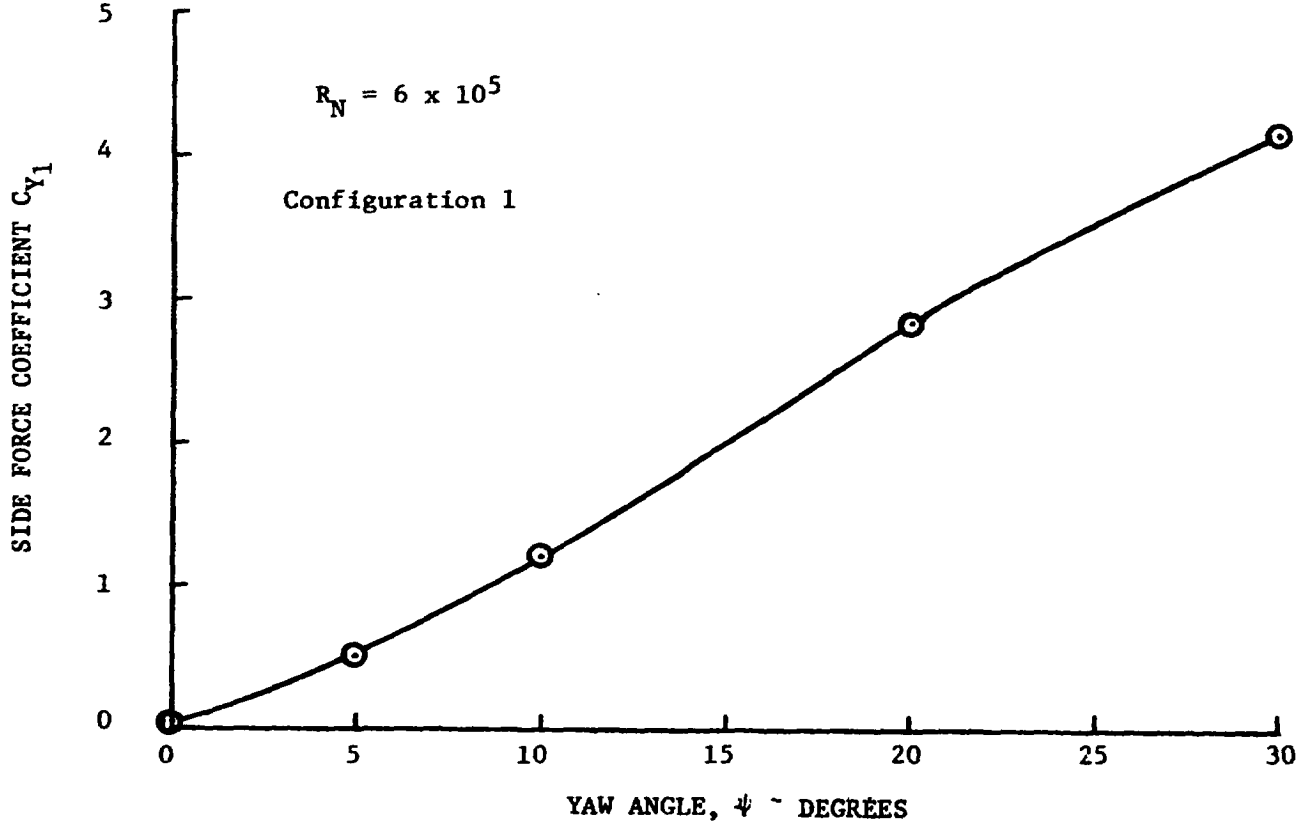

Figure 3.2.2 Effect of Wind Angle on Side Force Coefficient, C_{Y_1}

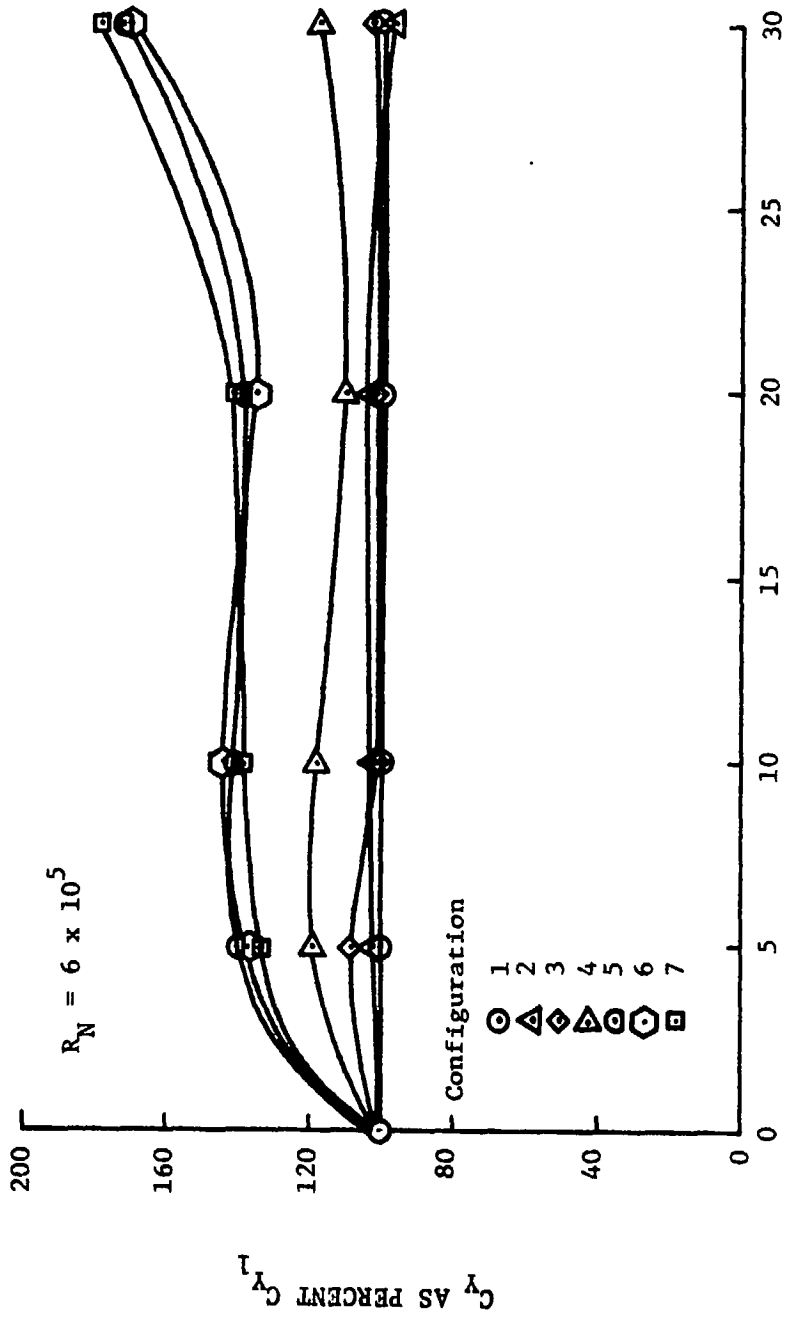

Figure 3.2.3 Comparison of Side Force Coefficients Configuration 1,2,3,4,5,6,7

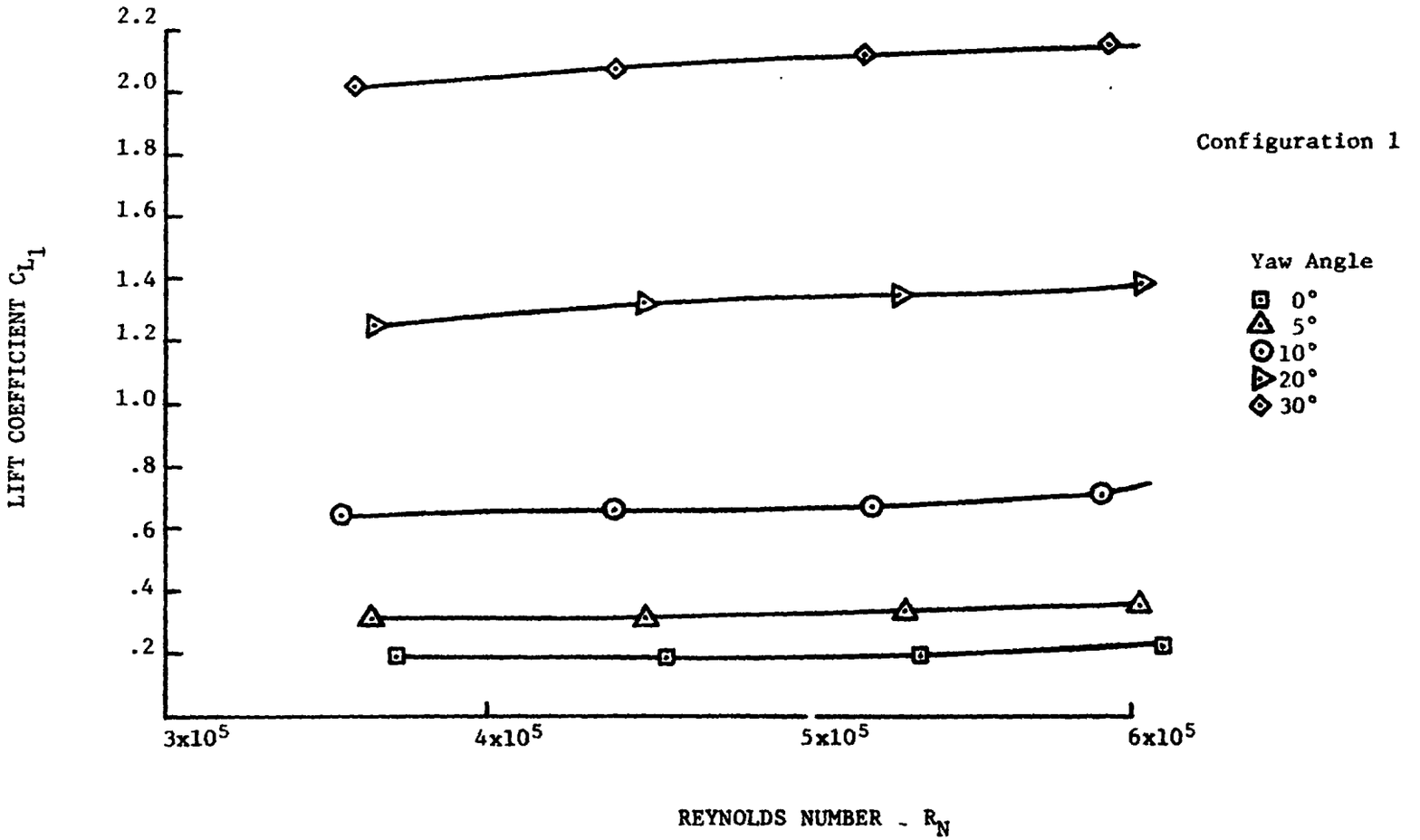

Figure 3.3.1 Reynolds Number Effect on Lift Coefficient, C_{L_1}

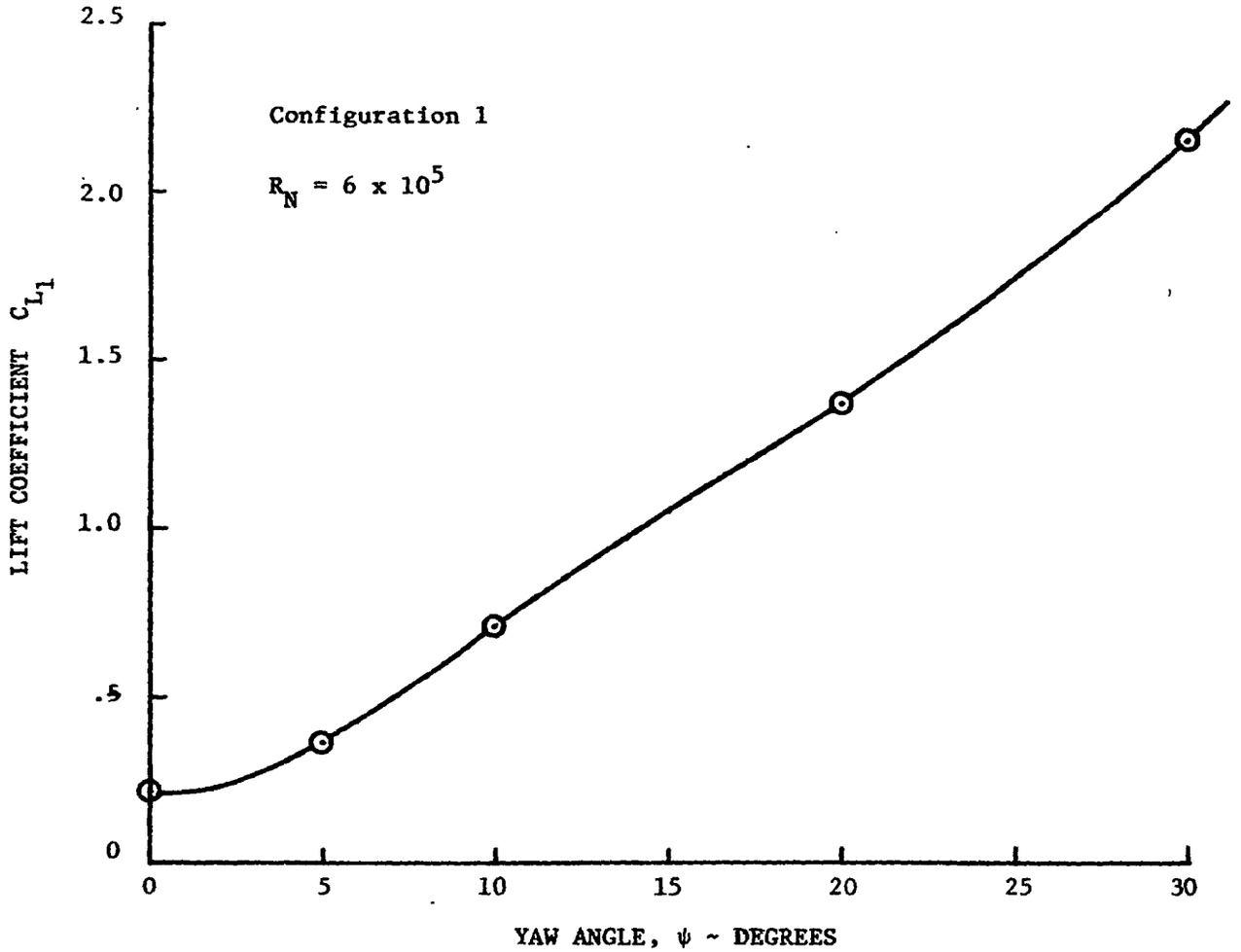

Figure 3.3.2 Effect of Wind Angle on Lift Coefficient, C_{L_1}

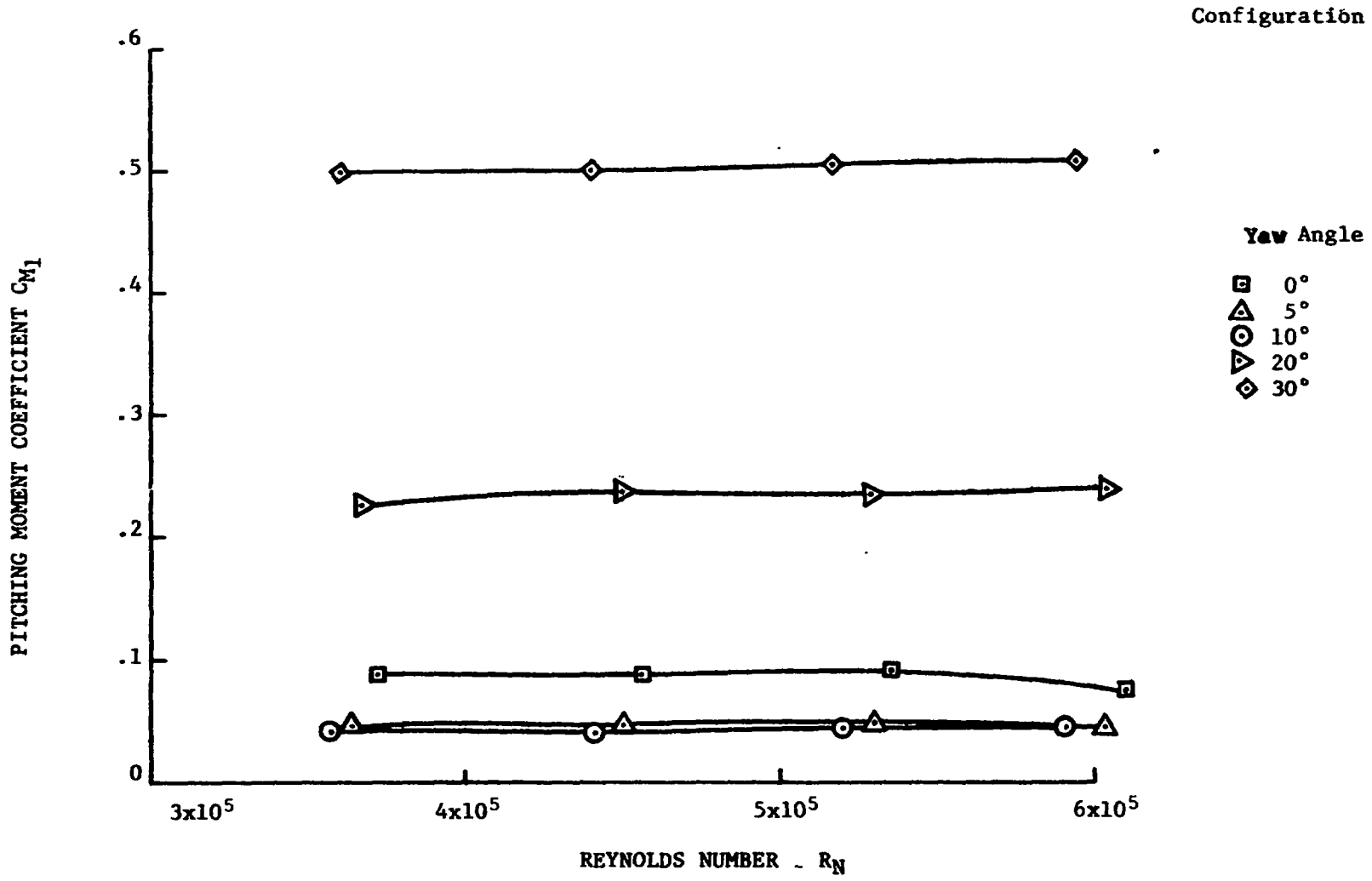

Figure 3.4.1 Reynolds Number Effect on Pitching Moment Coefficient, C_{M_1}

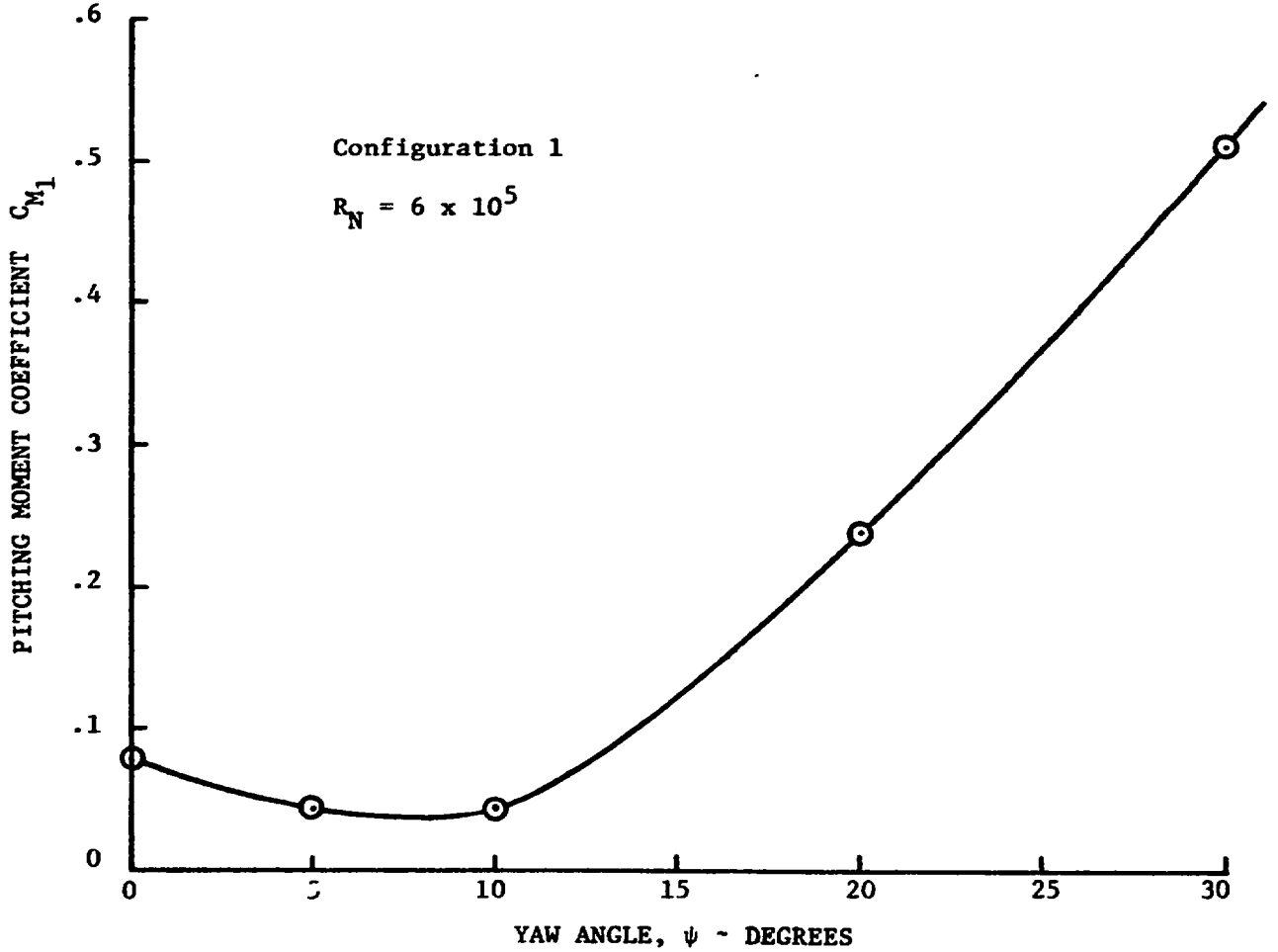

Figure 3.4.2 Effect of Wind Angle on Pitching Moment Coefficient, C_{M_1}

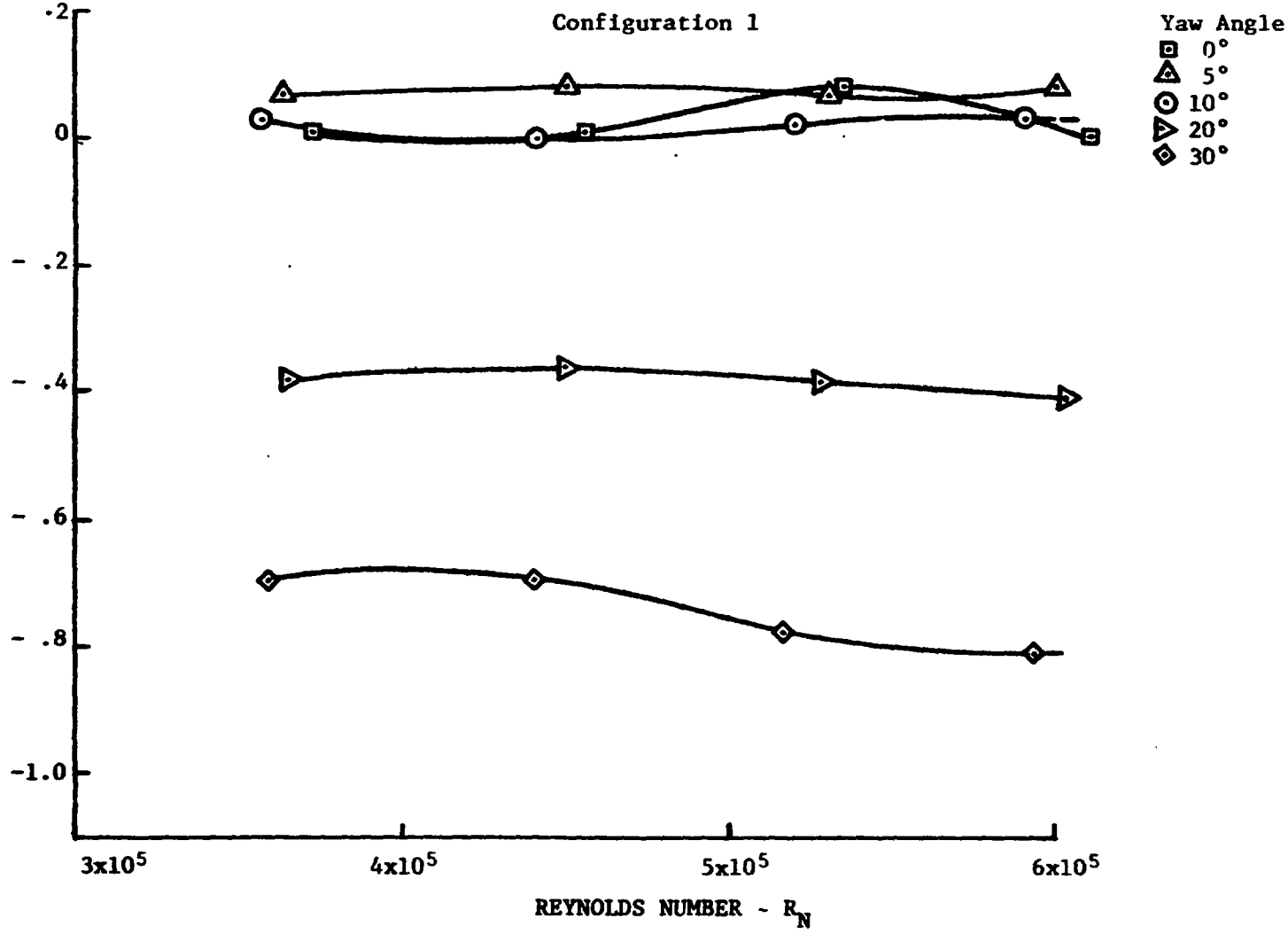

Figure 3.5.1 Reynolds Number Effect on Rolling Moment Coefficient, C_{ℓ_1}

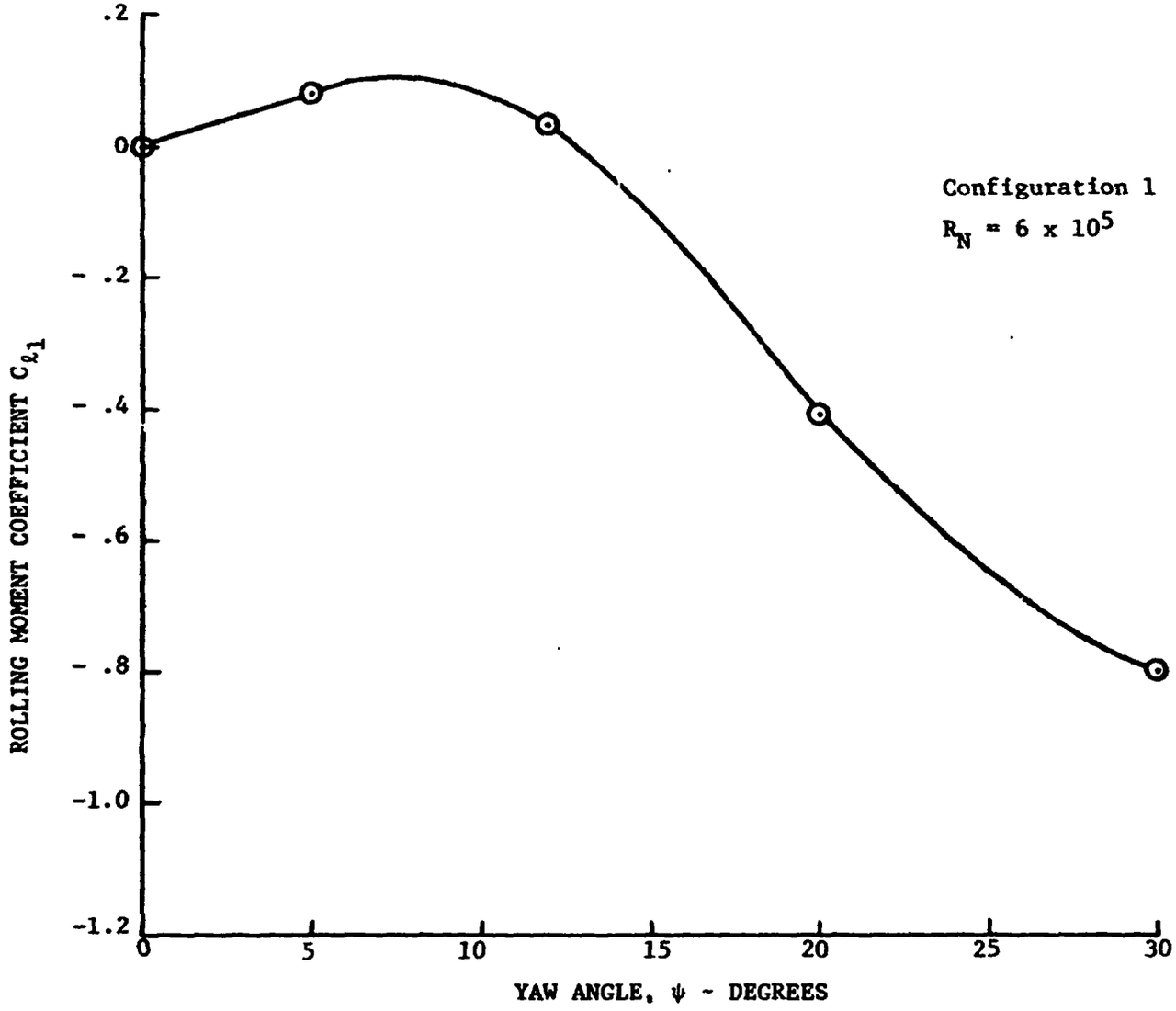

Figure 3.5.2 Effect of Wind Angle on Rolling Moment Coefficient C_{ℓ_1}

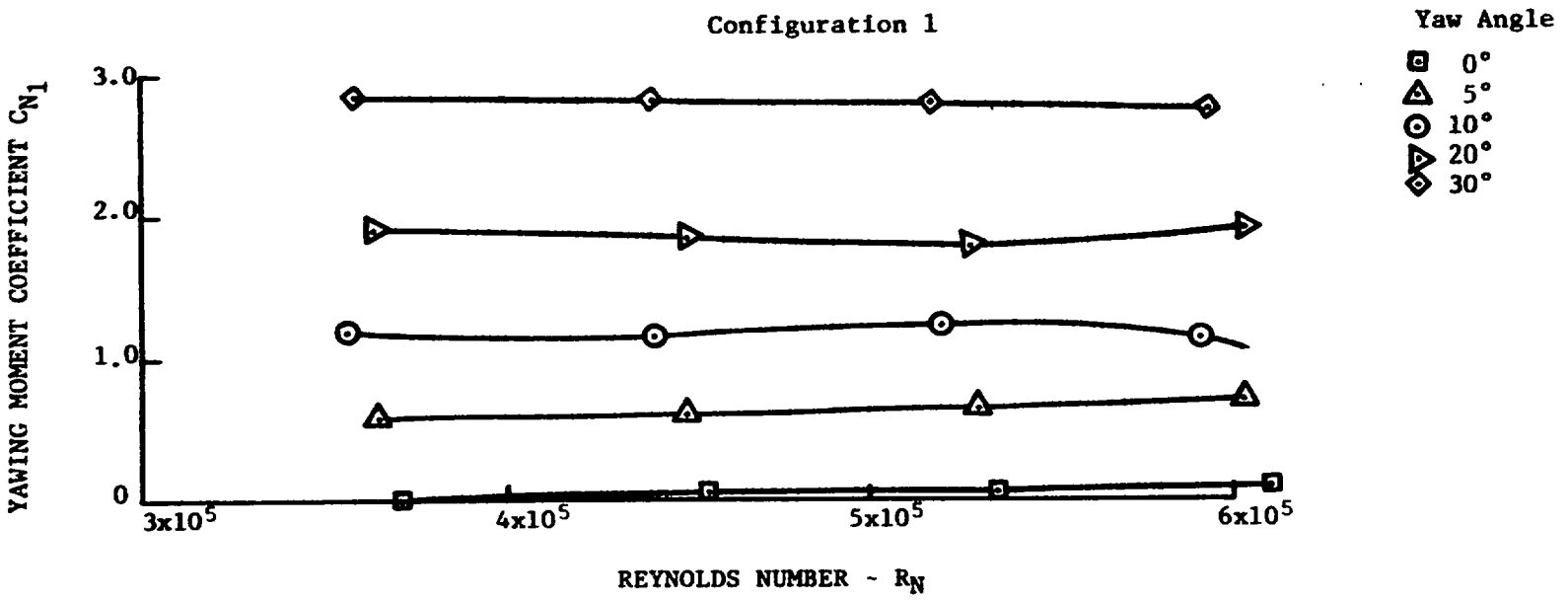

Figure 3.6.1 Reynolds Number Effect on Yawing Moment Coefficient, C_{N_1}

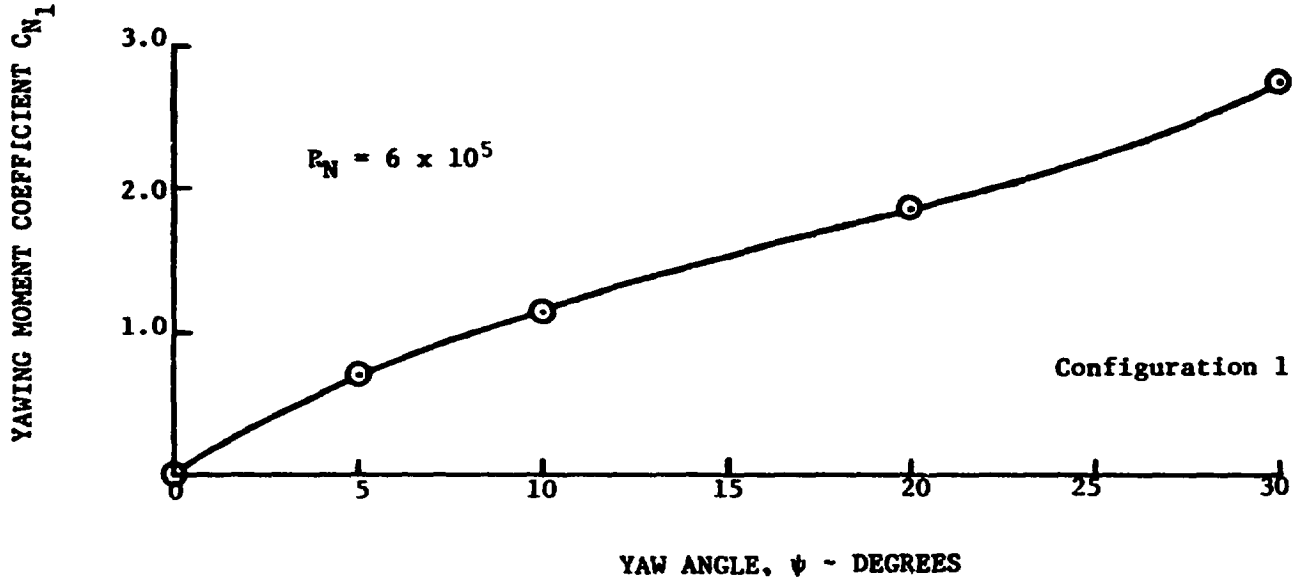

Figure 3.6.2 Effect of Wind Angle on Yawing Moment Coefficient C_{N_1}

Table I Full-scale basic vehicle characteristics

Tractor:

Make	White Freightliner
Year	1974
Type	Cab over engine(with sleeper)
Number of axles	3
Tire size	10.00-22
Engine -	
Type	350 Cummings Turbocharged
Model	NTC-350
Displacement, in^3	855
Horsepower at 2100 rpm	310
Transmission -	
Type	Fuller Roadranger
Model	RTO-9513

Trailer:

Make	Strick
Year	1972
Length, ft	45
Type	Smooth sidewall
Number of axles	2
Tire size	10.00-22

Table II Drag coefficients, $R_N = 6 \times 10^5$

Configuration	Yaw angles, ψ				
No.	0°	5°	10°	20°	30°
1	0.990	1.110	1.362	1.677	1.840
2	0.942	1.031	1.236	1.580	1.684
3	0.737	0.890	1.157	1.560	1.579
4	0.592	0.750	0.960	1.204	1.080
5	0.506	0.560	0.646	0.730	-----
6	0.458	0.470	0.515	0.420	0.290
7	0.400	0.407	0.420	0.420	0.270

Table III Influence on the drag coefficient by configuration changes and relative wind angle

CONFIGURATION				DRAG		
Part added	No.	Zero wind incremental decrease	Zero wind accumulative decrease	ΔC_D at [1] $\frac{}{C_{D_1}}$ $R_N 6 \times 10^5$	Average [2] incremental decrease	Average [2] accum. decrease
Cab nose	1 → 2	4.8%	4.8%	-4.8% -9.3%	7%	7%
Cab top	2 → 3	15.7%	20.5%	-1.2% -15.7%	9%	16%
Gap enclosure (Top & sides)	3 → 4	19.7%	40.2	-12.6% -21.2%	17%	33%
Lower side panels	4 → 5	8.7%	48.9	-8.7% -28.3%	19%	52%
Rear	5 → 6	4.8%	53.7	-4.8% -18.5%	10%	62%
Bottom (Cab & trailer)	6 → 7	5.9%	59.6%	0.0% -7.0%	5%	67%

1. Range of relative wind effects from Table II. (for $\psi = 0^0$ to $\psi = 20^0$).

2. Qualitative - relative winds from $\psi = 0^0$ to $\psi = 20^0$.

Table IV Comparison of tests run at Dryden Flight Research Center and the University of Kansas, for $\beta = 0$.

DFRC[1]	KU[2]	$C_{D,DFRC}$	$C_{D,KU}$ $R_N = 6 \times 10^5$	Difference %
Baseline	1	1.17	0.990	15.4%
	2		0.942	
Rounded front and gap enclosure	3		0.787	
	4	.74[3]	0.592[4]	20.0%
	5		0.506	
	6		0.458	
	7		0.400	

1. DFRC — Configurations run at Dryden Flight Research Center from References 3 and 7
2. KU — Configurations run at the University of Kansas
3. DFRC — Incremental decrease, $\Delta C_D = .43$, 36.7% of baseline
4. KU — Incremental decrease, $\Delta C_D = .398$, 40.2% of baseline

Table V Base pressure coefficients,

$R_N = 6 \times 10^5$

Configuration	Yaw angles, ψ				
No.	0°	5°	10°	20°	30°
1	-0.216	-0.315	-0.390	-0.500	-0.532
2	-0.222	-0.306	-0.390	-0.457	-0.515
3	-0.240	-0.297	-0.357	-0.469	-0.518
4	-0.243	-0.295	-0.363	-0.427	-0.494
5	-0.228	-0.239	-0.279	-0.396	-0.492
6	-0.084	-0.085	-0.087	-0.088	-0.181
7	-0.058	-0.058	-0.019	-0.032	-0.128

Table VI Side force coefficients,

$R_N = 6 \times 10^5$

Configuration	Yaw angles, ψ				
No.	0°	5°	10°	20°	30°
1	0.000	0.520	1.220	2.860	4.150
2	0.000	0.530	1.260	2.940	4.050
3	0.000	0.560	1.250	2.940	4.290
4	0.000	0.620	1.440	3.170	4.900
5	0.000	0.730	1.720	3.990	7.180
6	0.000	0.710	1.740	3.880	7.320
7	0.000	0.690	1.690	4.040	7.450

Table VII Influence on the side force coefficient by configuration changes

CONFIGURATION		SIDE FORCE		
Part added	No.	$\frac{\Delta C_Y}{C_{Y_1}} + R_N = 6 \times 10^5$	Average incremental change	Average accumulative change
Cab nose	1 → 2	- 2.4% + 3.3%	+ 1%	1%
Cab top	2 → 3	- 0.8% + 5.8%	+ 3%	4%
Gap enclosure (Top & sides)	3 → 4	0% + 14.7%	+13%	17%
Lower panels (Tractor & trailer)	4 → 5	0% + 54.9%	+32%	49%
Rear	5 → 6	- 3.8% + 3.4%	- 1%	48%
Bottom	6 → 7	-4.1% + 5.6%	- 0-	48%

Table VIII Lift coefficients, $R_N = 6 \times 10^5$

Configuration	Yaw angles, ψ				
No.	0°	5°	10°	20°	30°
1	0.215	0.359	0.710	1.370	2.152
2	0.220	0.395	0.729	1.485	2.258
3	0.040	0.141	0.420	1.285	2.145
4	0.020	0.121	0.397	1.240	2.363
5	0.137	0.349	0.787	2.280	3.450
6	0.240	0.460	0.940	2.460	3.300
7	0.135	0.310	0.740	2.015	2.815

Table IX Pitching moment coefficients,
$R_N = 6 \times 10^5$

Configuration	Yaw angles, ψ				
No.	0 °	5 °	10 °	20 °	30 °
1	0.078	0.045	0.043	0.238	0.510
2	0.147	0.094	0.004	0.196	0.448
3	0.018	0.010	0.084	0.291	0.428
4	0.010	0.025	0.087	0.326	0.390
5	0.011	0.020	0.101	0.334	0.398
6	0.063	0.105	0.194	0.391	0.260
7	0.071	0.079	0.115	0.290	0.147

Table X Rolling moment coefficients,
$R_N = 6 \times 10^5$

Configuration	Yaw angles, ψ				
No.	0 °	5 °	10 °	20 °	30 °
1	0.000	0.081	0.030	-0.411	-0.800
2	0.000	0.089	0.139	-0.390	-0.739
3	0.000	0.060	-0.043	-0.330	-0.501
4	0.000	0.045	-0.093	-0.363	-0.663
5	0.000	0.061	-0.071	-0.540	-1.040
6	0.000	-0.044	-0.172	-0.555	-0.605
7	0.000	-0.026	-0.125	-0.486	-0.585

Table XI Yawing moment coefficients, $R_N = 6 \times 10^5$

Configuration No.	Yaw angles, ψ 0°	5°	10°	20°	30°
1	0.000	0.690	1.120	1.830	2.710
2	0.000	0.540	0.705	1.610	2.510
3	0.000	0.450	0.380	1.400	2.050
4	0.000	0.080	0.195	0.180	0.980
5	0.000	0.062	1.240	2.030	0.390
6	0.000	0.998	1.660	2.170	1.070
7	0.000	1.230	1.790	2.470	1.320

7. APPENDIX

POWER REQUIRED

The model data for configuration 1 were applied to the full size prototype vehicle at road speed of 88.5 km/hr. (55 mph). The wind component was rotated from 0° to 180° β. Wind speeds used were 0, 18km/hr. (11.2 mph), 36 km/hr. (22.4 mph).

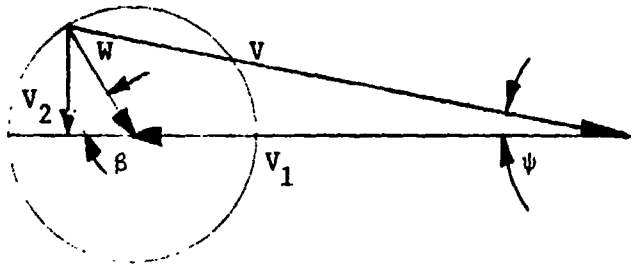

V = Relative wind speed

V_1 = Ground speed

W = Actual wind velocity

V_2 = Side wind velocity component

β = Wind angle relative to the vehicle path

ψ = Relative wind angle

7.1 Power to Overcome Aerodynamic Drag - configuration 1

The power required is:

$$P = \frac{D\ V_1}{1000} \text{ kw (Multiply by 1.341 = hp)}$$

where

$D = 1/2\ \rho\ V^2\ C_D A$

$A = 8.724\ m^2$ (94 ft^2)

$\rho = 1.226\ kg/m^3$ (.002378 $slugs/ft^3$)

C_D is taken from Figure 3.1.2 for configuration 1 at approximate values of ψ.

Example:

$V_1 = 88.5$ km/hr. or 24.58 m/sec. (55 mph)

$W = 18$ km/hr. or 5.0 m/sec (11.2 mph)

$\beta = 15°$

$\psi = 2.52°$

From Figure 3.1.2:

$C_{D_1} = 1.033$

Then:

$D = 1/2 \times 1.226 \times (29.42)^2\ (1.033)\ (8.724)$

$D = 4781.5$ N(1074.9 lb.)

$$P = \frac{(4781.5)\ \ (24.58)}{1000} = 117.5 \text{ kw}$$

P = 117.5 kw (157.6 hp) (plotted in Figure 3.1.10)

7.2 Power Required for Other Configurations

To find the power required for any other configuration:

1. Determine relative wind speed V and the relative wind angle ψ.
2. Go to Figure 3.1.3. Find the percentage of C_{D_X} this configuration has of C_{D_1}.
3. Go to the power graph, Figure 3.1.10, and locate the power required for configuration 1 at the wind angle β.
4. Multiply this value of power with C_{D_X} / C_{D_1} and the power required for this configuration X is obtained.

Example:

1. Configuration 7

Wind speed W = 18 km/hr. (11.2 mph)

Wind angle $\beta = 15°$

Relative wind angle ψ:

$$\psi = \text{Tan}^{-1} \frac{W \sin \beta}{V_1 + W \cos \beta}$$

$$\psi = \text{Tan}^{-1} \frac{18 \text{ km/hr. } \sin 15°}{88.5 \text{ km/hr. } + 18 \text{ km/hr. } \cos 15°}$$

$$\psi = 2.52°$$

From Figure 3.1.3:

$$\frac{C_{D_7}}{C_{D_1}} = 38.9\% = \frac{P_7}{P_1}$$

From Figure 3.1.10:

$P_1 = 117.5$ kw (157.6 hp) and $P_7 = 45.7$ kw (61.3 hp)